Test of QED

≡ measurement of the electromagnetic fine structure constant α in differnt systems

1) High energy range, accessible with particle colliders

2) Low energy range, accessible with small experiments
   (magnetic moment of the electron → most precise test of QED)

3) Condensed matter systems (quantum Hall effect, Josephson effect)

$$e^+e^- \rightarrow \mu^+\mu^-$$

Only s-channel possible, thus need to take interference with Z into account

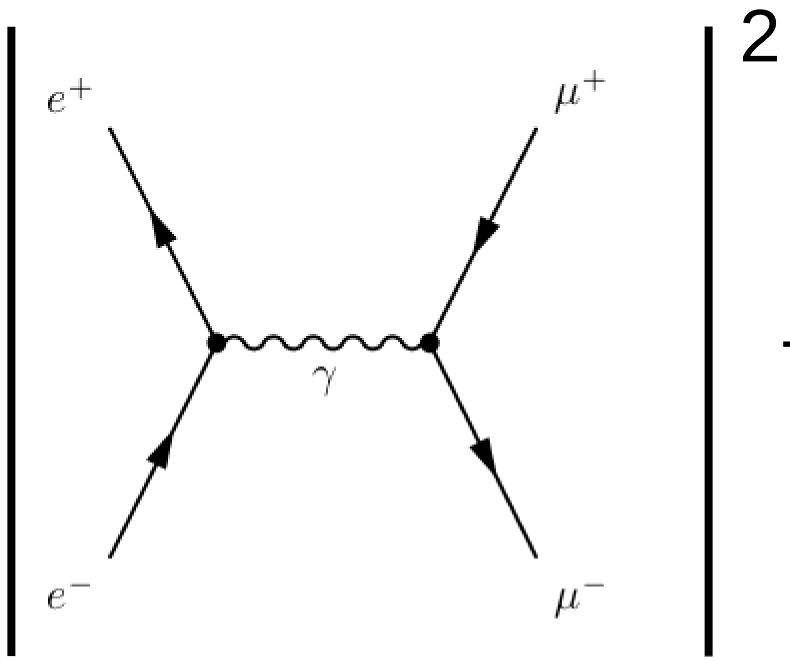

+ interference +

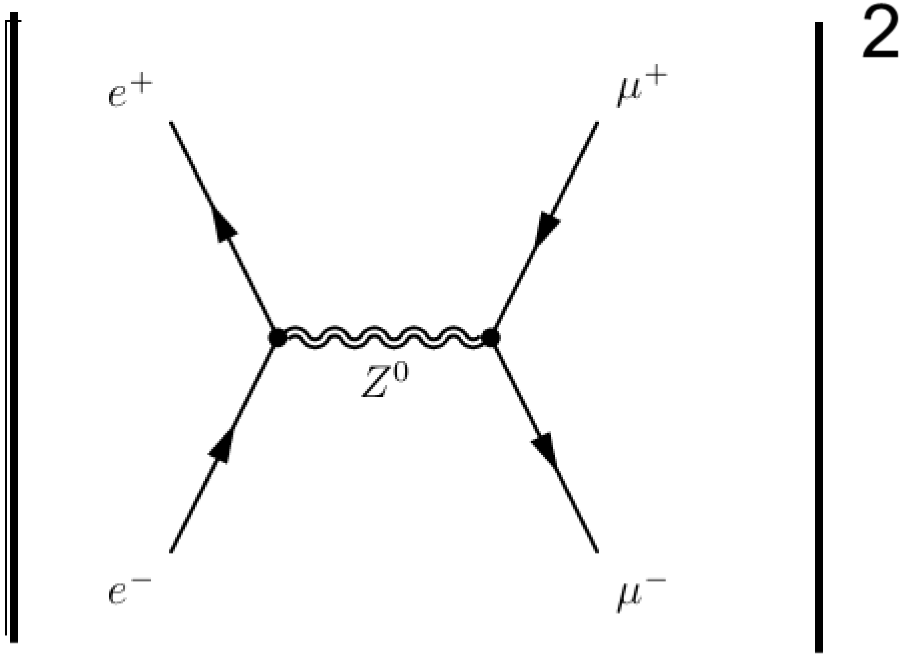

Limits of QED

Possible deviation from QED:
Additonal heavy photon

$$\frac{1}{r} \rightarrow \frac{1}{r}(1 - e^{-\Lambda r})$$

$$\frac{1}{q^2} \rightarrow \frac{1}{q^2}(1 + \frac{q^2}{\Lambda^2}) = \frac{1}{q^2}F(q^2)$$

$$\sigma^{e^+e^- \rightarrow \mu^+\mu^-} \rightarrow \frac{4\pi\alpha^2}{3s}(1 \pm \frac{s}{\Lambda^2 - s})^2$$

Λ corresponds to the mass of the new photon

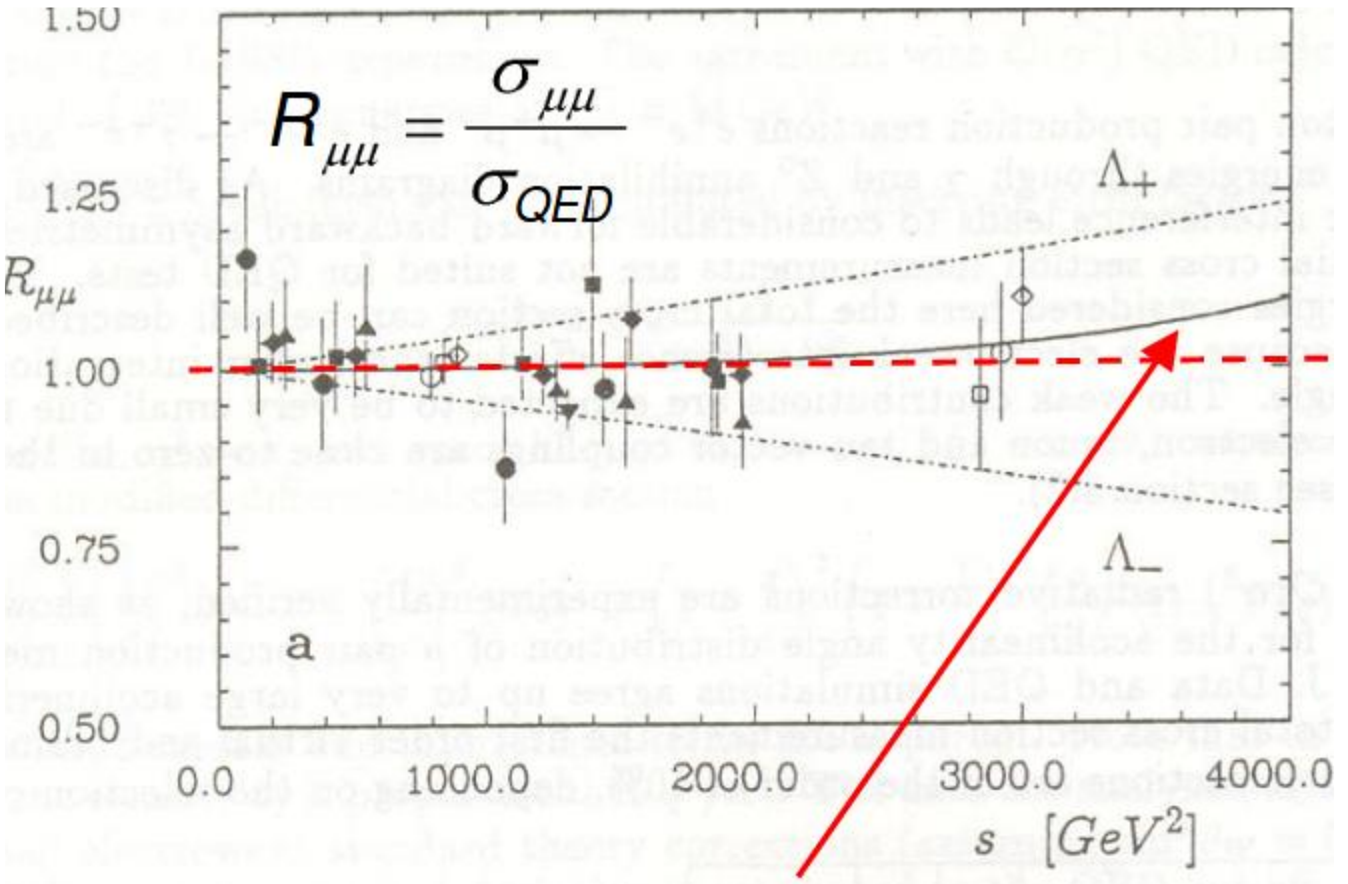

$$\frac{\sigma_{\mu\mu}^{\gamma+Z}}{\sigma_{QED}}$$

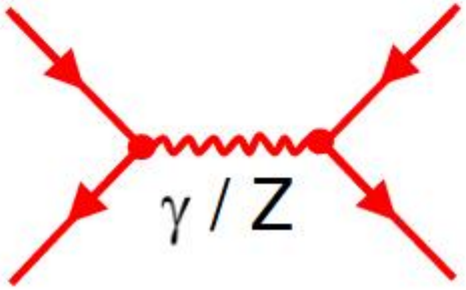

Λ > 200 GeV
→ confirms „Coulomb law"
& point-like nature of electron down to 10^{-18} m

Limits of QED

Similar tests have been performed in Bhabha scattering

Form factor modifies differential cross section:

$$\frac{d\sigma}{d\Omega} = \frac{\alpha^2}{2s}\left(\frac{u^2+s^2}{t^2}\left|F(t)\right|^2 + \frac{2u^2}{ts}\left|F(t)F(s)\right| + \frac{u^2+t^2}{s^2}\left|F(s)\right|^2\right)$$

t-channel interference s-channel

Tasso: $\Lambda_+ > 370$ GeV

$\Lambda_- > 190$ GeV

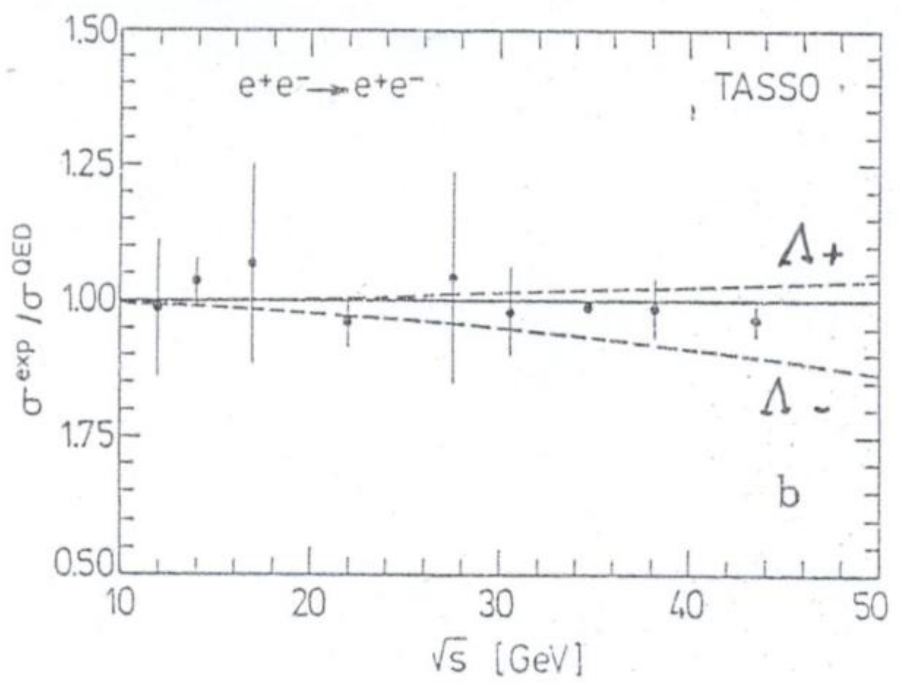

Combined PETRA result:

$\Lambda^+ > 435\ \mathrm{GeV\ at}\ 95\%$ CL

$\Lambda^- > 590\ \mathrm{GeV\ at}\ 95\%$ CL

Test of radiative corrections

Emission of photon in final state
→ final state particle are not
anymore back-to-back

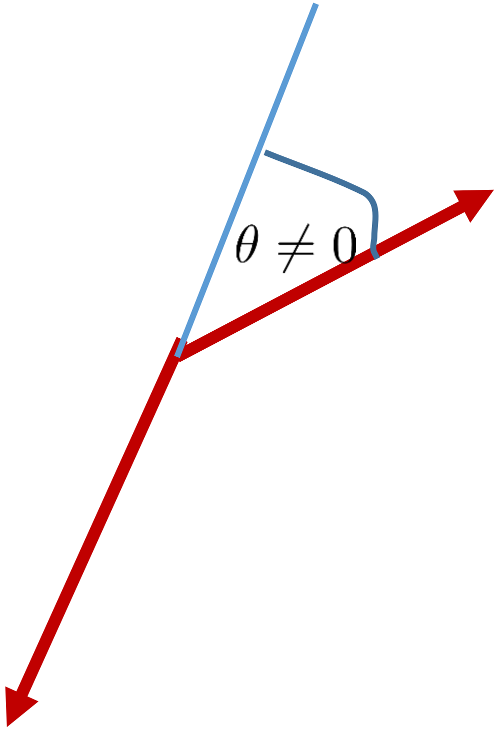

s- and t-channel

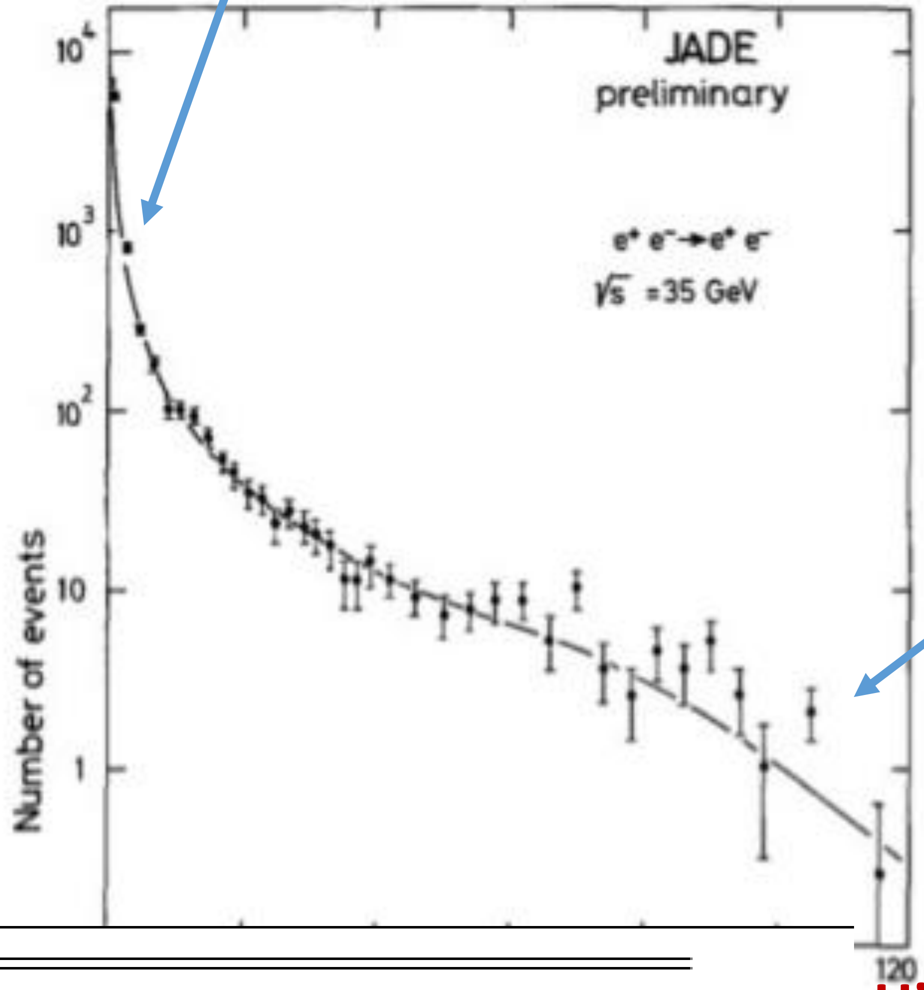

radiative
corrections

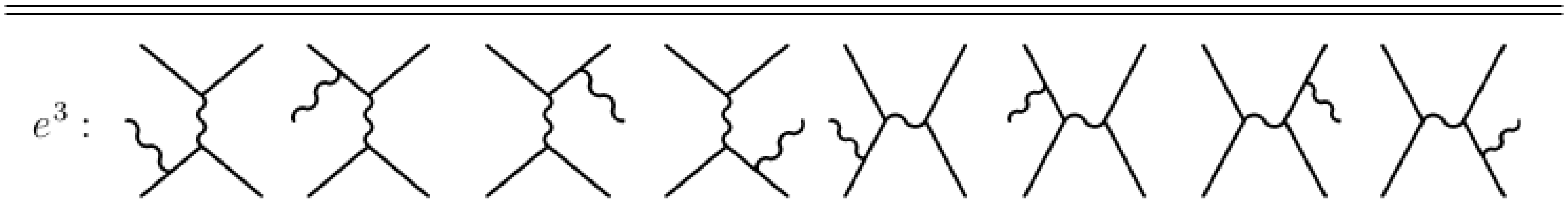

Higher order corrections describe well data!

Discovery of the Tau Lepton

MARK I (SLAC), 1975 M. Pearl et al.
Nobel Prize 1995 for M. Pearl

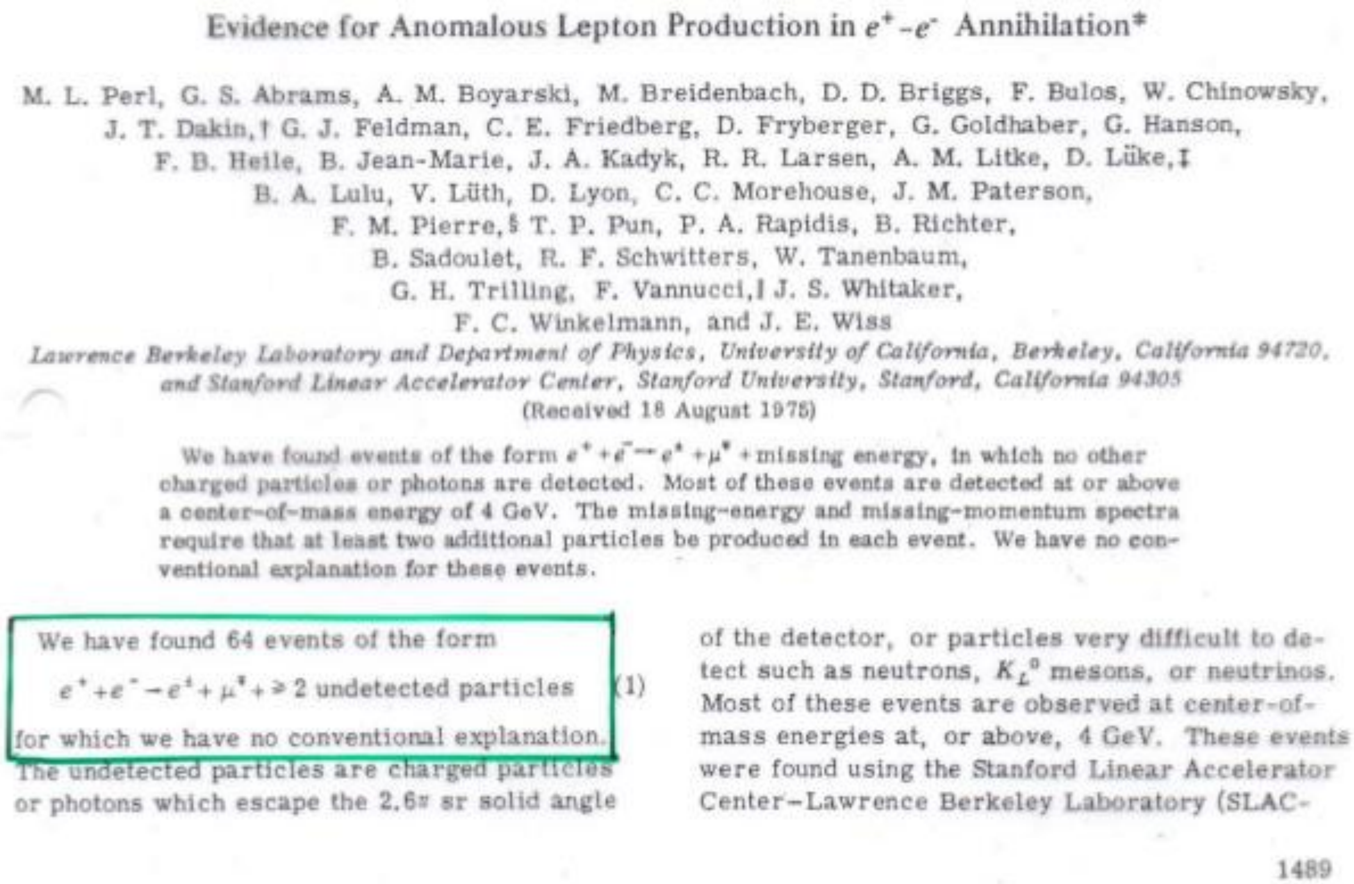

Evidence for Anomalous Lepton Production in e^+-e^- Annihilation*

M. L. Perl, G. S. Abrams, A. M. Boyarski, M. Breidenbach, D. D. Briggs, F. Bulos, W. Chinowsky, J. T. Dakin,† G. J. Feldman, C. E. Friedberg, D. Fryberger, G. Goldhaber, G. Hanson, F. B. Heile, B. Jean-Marie, J. A. Kadyk, R. R. Larsen, A. M. Litke, D. Lüke,‡ B. A. Lulu, V. Lüth, D. Lyon, C. C. Morehouse, J. M. Paterson, F. M. Pierre,§ T. P. Pun, P. A. Rapidis, B. Richter, B. Sadoulet, R. F. Schwitters, W. Tanenbaum, G. H. Trilling, F. Vannucci,‖ J. S. Whitaker, F. C. Winkelmann, and J. E. Wiss

Lawrence Berkeley Laboratory and Department of Physics, University of California, Berkeley, California 94720, and Stanford Linear Accelerator Center, Stanford University, Stanford, California 94305

(Received 18 August 1975)

We have found events of the form $e^+ + e^- \to e^\pm + \mu^\mp$ + missing energy, in which no other charged particles or photons are detected. Most of these events are detected at or above a center-of-mass energy of 4 GeV. The missing-energy and missing-momentum spectra require that at least two additional particles be produced in each event. We have no conventional explanation for these events.

We have found 64 events of the form

$$e^+ + e^- \to e^\pm + \mu^\mp + \geq 2 \text{ undetected particles} \quad (1)$$

for which we have no conventional explanation. The undetected particles are charged particles or photons which escape the 2.6π sr solid angle of the detector, or particles very difficult to detect such as neutrons, K_L^0 mesons, or neutrinos. Most of these events are observed at center-of-mass energies at, or above, 4 GeV. These events were found using the Stanford Linear Accelerator Center–Lawrence Berkeley Laboratory (SLAC-

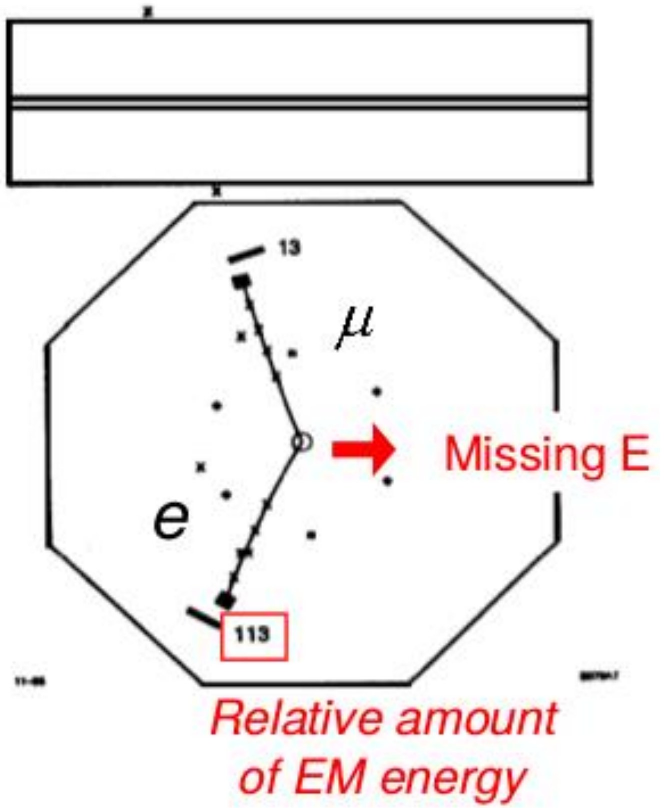

Explanation:

$$e^+e^- \to \tau^+ \tau^-$$

$\tau^- \to e^- \bar{\nu}_e \nu_\tau$

$\tau^+ \to \mu^+ \nu_\mu \bar{\nu}_\tau$

A lot of Discussions in 1975:

Are these events really decays of a new 3rd generation of heavy lepton ?

$$e^+e^- \to q\bar{q}$$

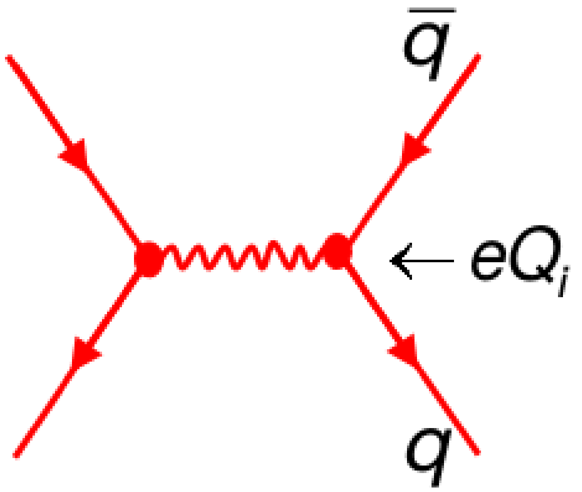

e^+e^- annihilation to a pair of quarks with subsequent hadronization.

$$Q_i = \begin{cases} +\frac{2}{3} \\ -\frac{1}{3} \end{cases}$$

Quarks have fractional charges and carry "color" as additional quantum number.

Additional color factor N_C

$$\left.\frac{d\sigma}{d\Omega}\right|_{ee\to hadrons} = \frac{\alpha^2}{4s} \cdot N_C \cdot \sum_{quarks\,i} Q_i^2 (1+\cos^2\theta)$$

Sum over kinematically possible quark flavors: $4m_q^2 < s$

$\sqrt{s}$	Quarks
< ~3 GeV	uds
< ~10 GeV	udsc
< ~350 GeV	udscb
> ~350 GeV	udscbt

From Quarks to Jets

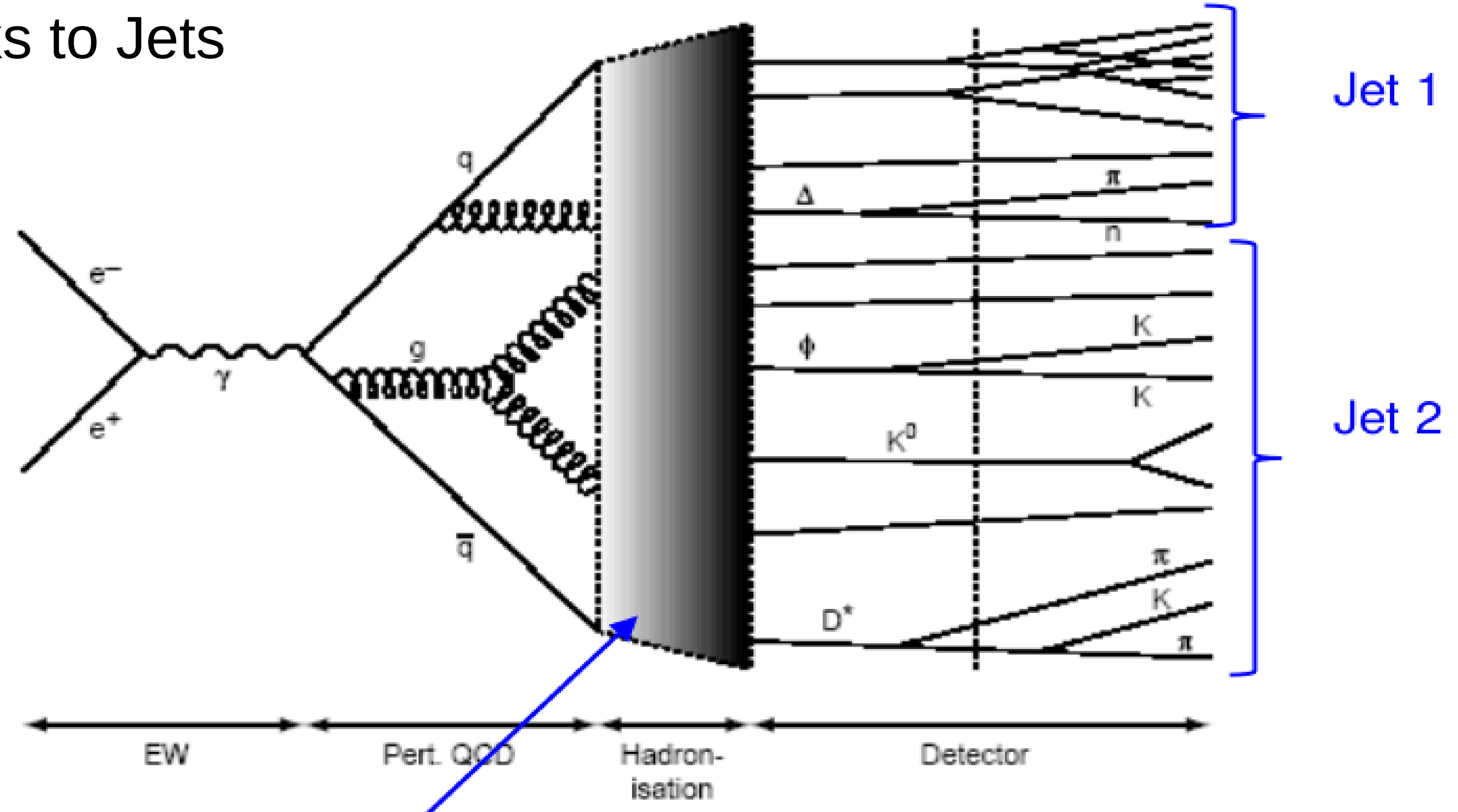

Described successfully by different phenomenological fragmentation models realized as Monte Carlo programs:
PHYTIA, HERWIG, SHERPA

~ 20 particles at 90 GeV

Quark jets and angular distribution

TASSO / PETRA

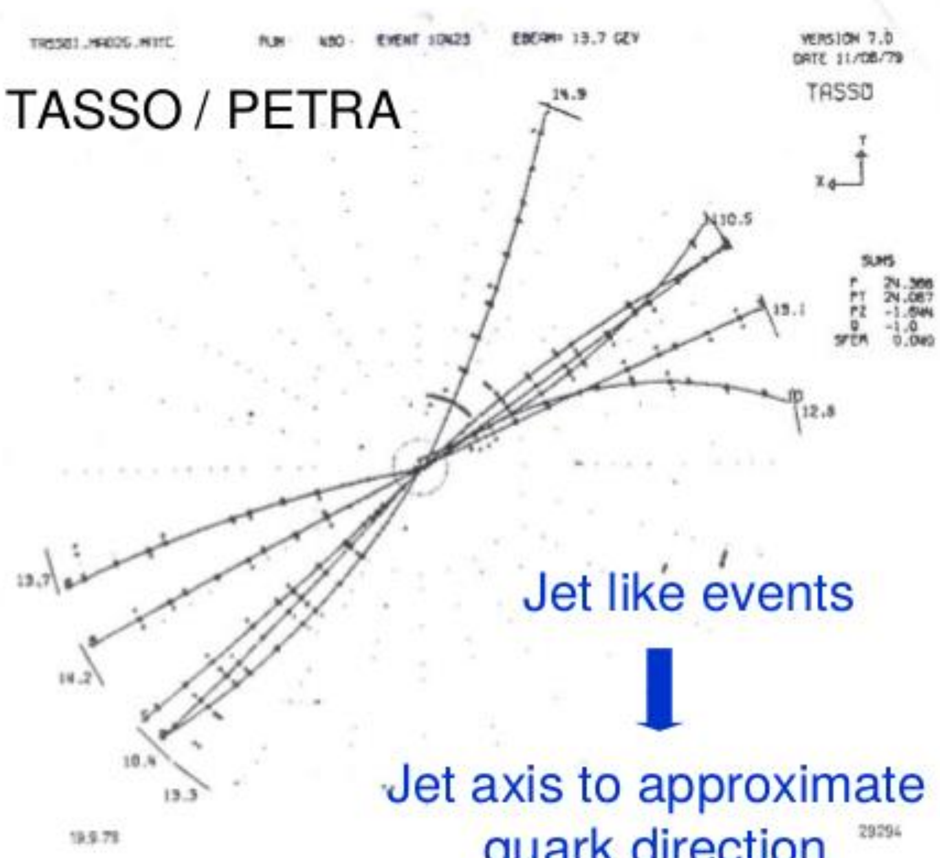

Jet like events

⬇

Jet axis to approximate quark direction

Fig.2 A typical multihadron event at 27.4 GeV recorded in the central detector. The inner 4 layers belong to the proportional chamber, the following 9 are zero degree layers of the drift chamber. The solid bars at the periphery mark time-of-flight counters.

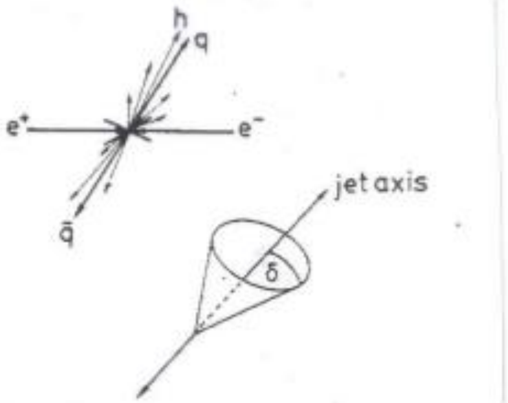

Not very convincing

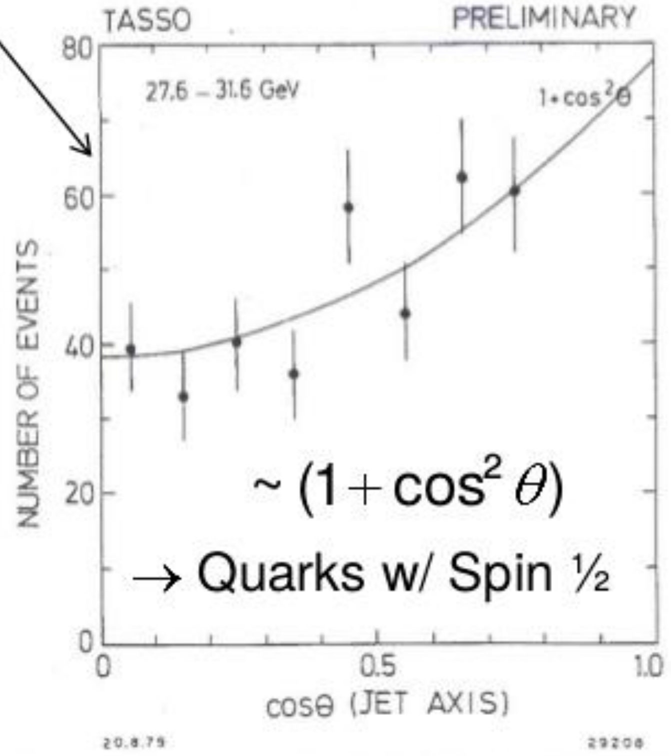

$\sim (1+\cos^2\theta)$

$\rightarrow$ Quarks w/ Spin ½

Fig.7 Angular distribution of the jet axis with respect to the beam.

Definition:

$$R_{had} = \frac{\sigma(ee \to hadrons)}{\sigma(ee \to \mu\mu)} = 3 \cdot \sum_i Q_i^2$$

$\sqrt{s}$	Quarks	$R_{had} = 3 \cdot \sum_i Q_i^2$
< ~3 GeV	uds	3·6/9=2.00
< ~10 GeV	udsc	3·10/9=3.33
< ~350 GeV	udscb	3·11/9=3.67
> ~350 GeV	udscbt	3·15/9=5.00

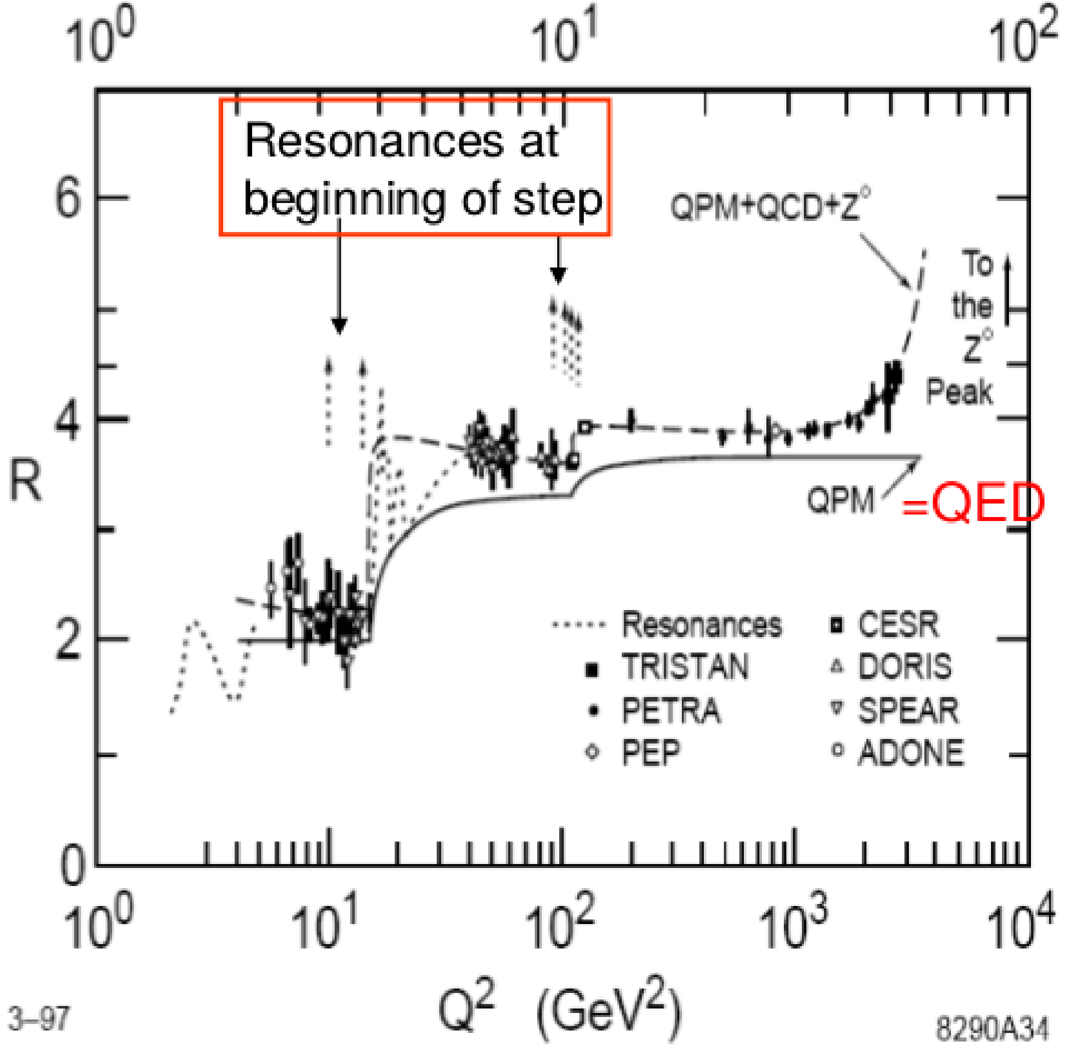

Data lies systematically higher than the prediction from Quark Parton Model (QPM) → gluon bremsstrhl.

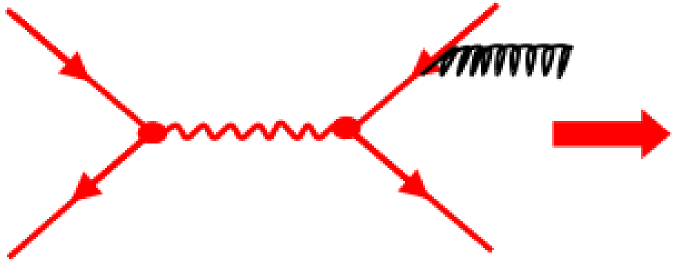

$$\sigma^{qq}(s) = \sigma^{qq}_{QED}(s)\left[1 + \frac{\alpha_s(s)}{\pi} + 1.411 \cdot \frac{\alpha_s(s)^2}{\pi^2} + \ldots\right]$$

~ 7%

Anomalous Magnetic Moment of the Electron

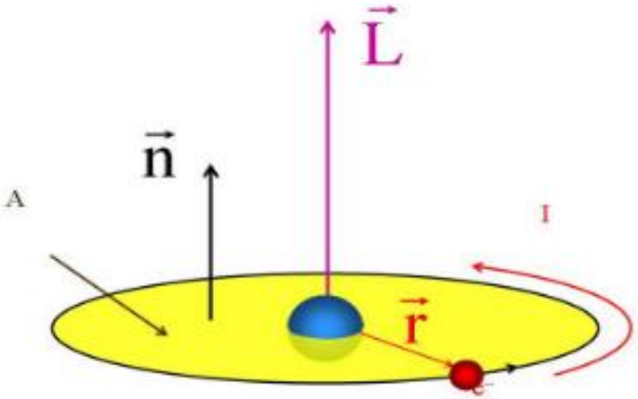

Classic magnetic moment

$$\vec{\mu}_l = \frac{q}{2m}\vec{L}$$

Quantum magnetic analogy

$$\vec{\mu_s} = g\frac{q}{2m}\vec{s} = -\frac{g}{2}\frac{e}{2m}$$

for Dirac particles lowest order QED: g = 2

Anomalous magnetic moment

$$\frac{g}{2} = 1 + a_{QED}(\alpha) + a_{hadronic} + a_{weak} + a_{new}$$

$$a \equiv \frac{g-2}{2}$$

negligible in SM

need fourth order loop correction (891 terms) to match experimental precision

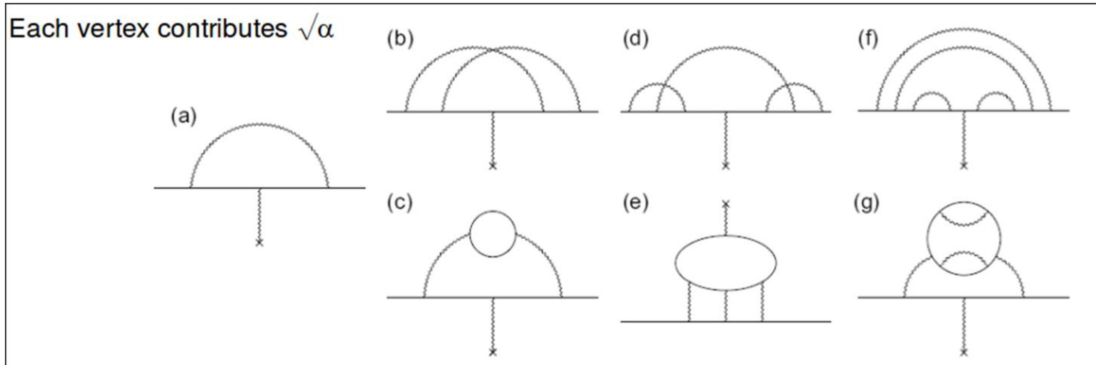

Figure 1.2: The second-order Feynman diagram (a), 2 of the 7 fourth-order diagrams (b,c), 2 of 72 sixth-order diagrams (d,e), and 2 of 891 eighth-order diagrams (f,g).

Penning Trap

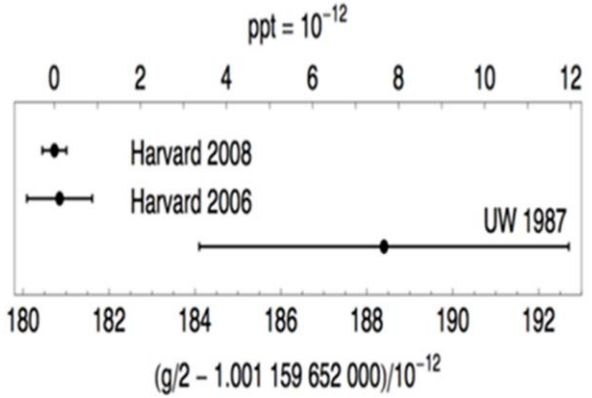

Gabrielse et al.,
Harvard University

Penning Trap Concept

(shown polarisation to trap positively charged ions)

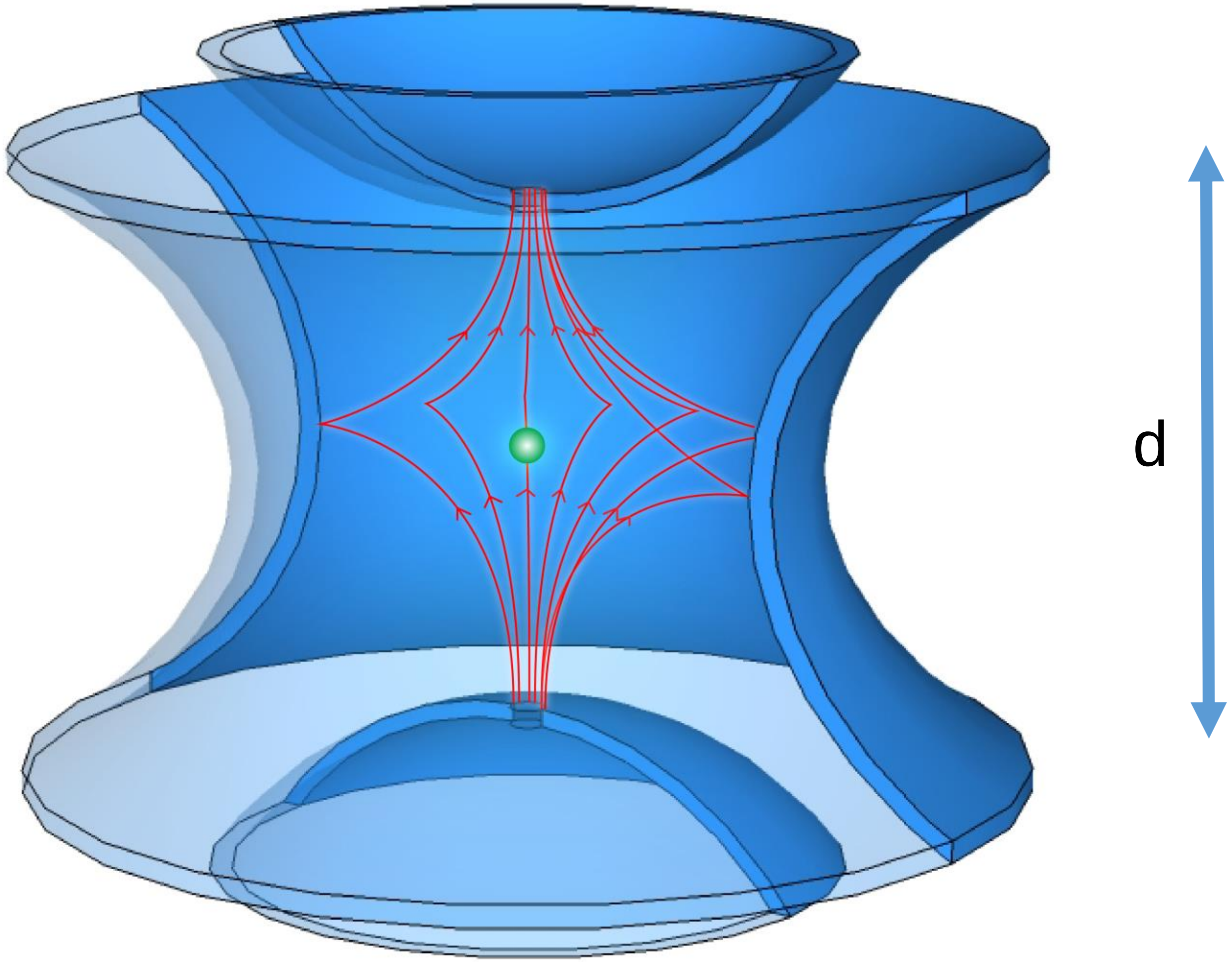

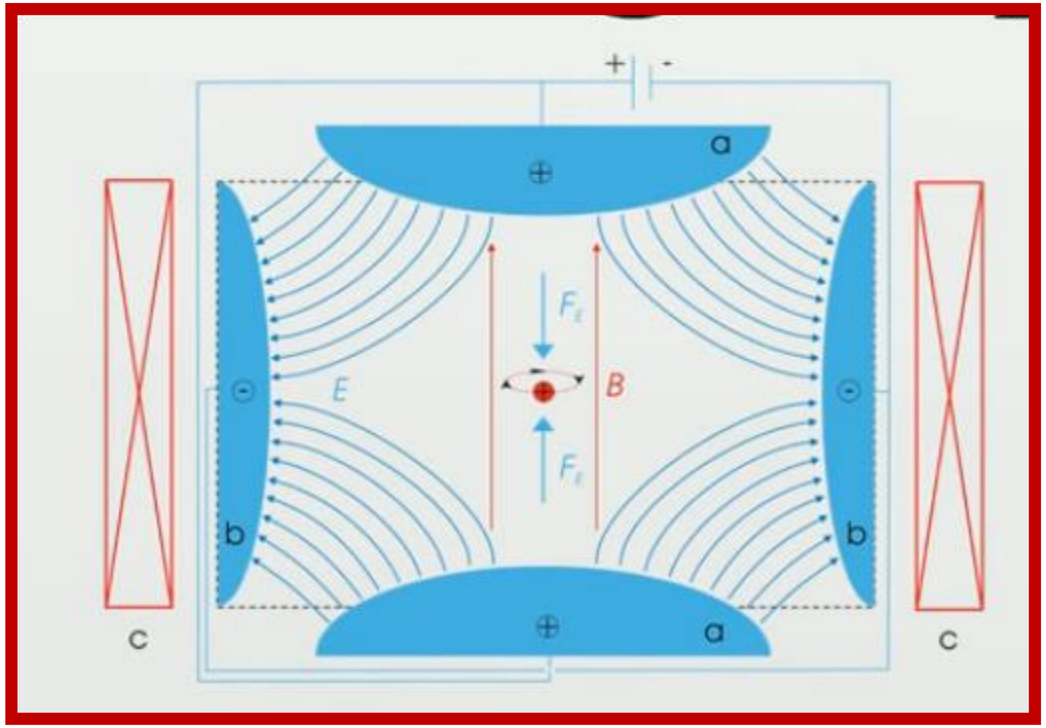

Motion of Electron in the Pening Trap

Due to electric field no pure cyclotron motion anymore

Composition of three oscillations

Axial motion $$\nu_z = \sqrt{\frac{eU}{Md^2}}$$ (200 MHz)

Modified cyclotron motion (150 GHz) $$\overline{\nu_c} = \nu_c - \frac{U}{2d^2 B}$$

Mangetron motion (133 kHz) $$\nu_m = \frac{U}{2d^2 B}$$

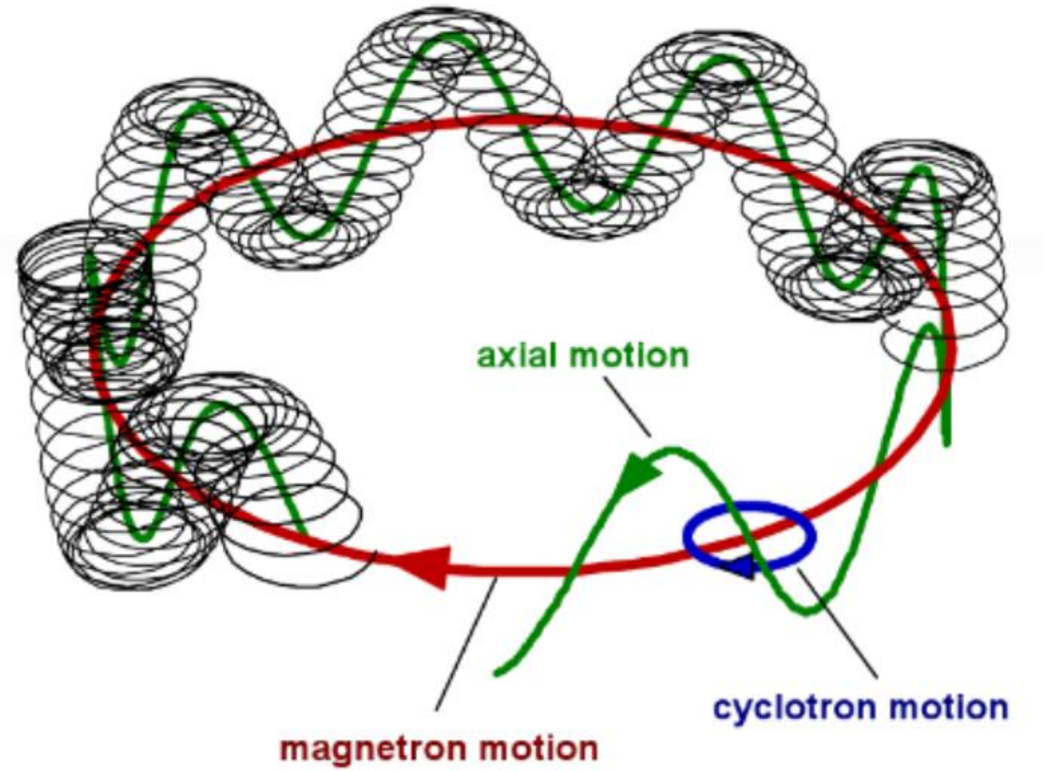

Non-relativistic electron in a magnetic field has the following energy levels:

$$E(n, m_s) = \frac{g}{2} h\nu_c m_s + (n + \frac{1}{2}) h\nu_c$$

Zeeman shift

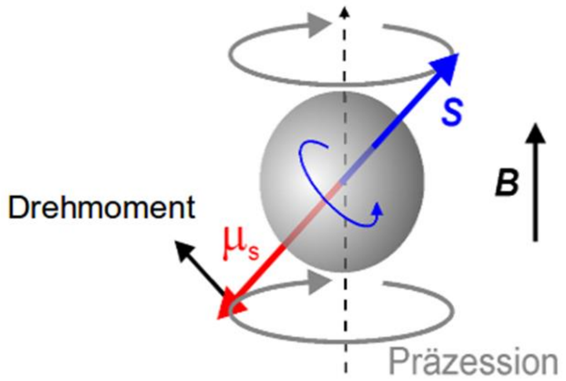

$$\vec{M} = \vec{\mu} \times \vec{B}$$

$$\nu_L = g \frac{eB}{4\pi m}$$

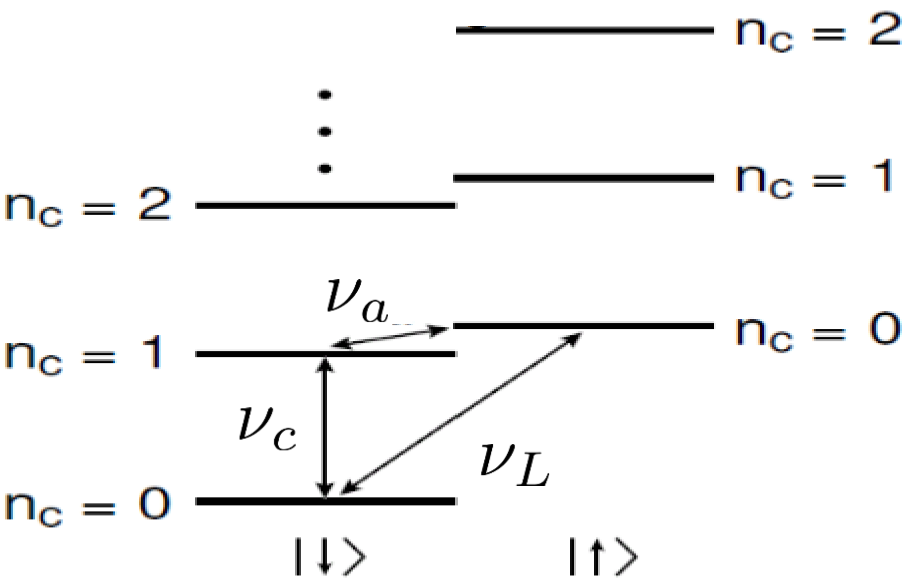

$$\nu_c = \frac{eB}{2\pi m}$$

$$\frac{g}{2} = \frac{\nu_L}{\nu_c} = 1 + \frac{\nu_L - \nu_c}{\nu_c} \equiv 1 + \frac{\nu_a}{\nu_c}$$

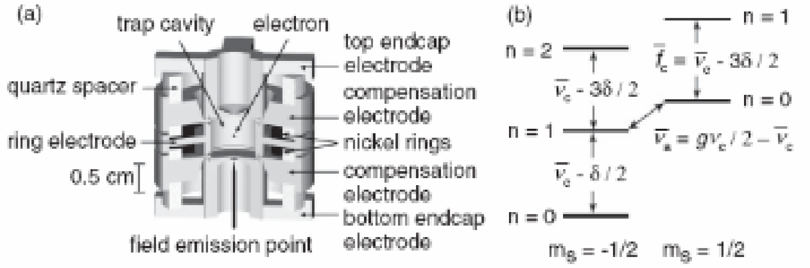

FIG. 2. Cylindrical Penning trap cavity used to confine a single electron and inhibit spontaneous emission (a), and the cyclotron and spin levels of an electron confined within it (b).

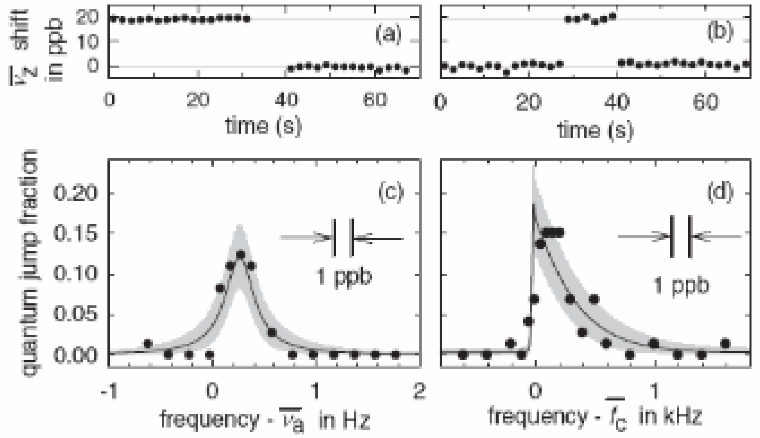

FIG. 3. Sample $\bar{\nu}_z$ shifts for a spin flip (a) and for a one-quantum cyclotron excitation (b). Quantum jump spectroscopy line shapes for anomaly (c) and cyclotron (d) transitions, with a maximum likelihood fit to the calculated line shapes (solid). The bands indicate 68% confidence limits for distributions of measurements about the fit values.

would damp in ~0.1 s via synchrotron radiation in free space. This spontaneous emission is greatly inhibited in the trap cavity (to 6.7 or 1.4 s here) when **B** is tuned so $\bar{\nu}_c$ is far from resonance with cavity radiation modes [7,15]. Blackbody photons that would excite the cyclotron ground state are eliminated by cooling the trap and vacuum enclosure below 100 mK with a dilution refrigerator [6]. (Thermal radiation through the microwave inlet makes <1 excitation/h.) The axial motion, damped by a resonant circuit, cools below 0.3 K (from 5 K) when the axial detection amplifier is off for crucial periods. The magnetron motion radius is minimized with axial sideband cooling [15].

For the first time, g is deduced from observed transitions between only the lowest of the spin ($m_s = \pm 1/2$) and cyclotron ($n = 0, 1, 2, \ldots$) energy levels [Fig. 2(b)],

$$E(n, m_s) = \frac{g}{2} h \nu_c m_s + \left(n + \frac{1}{2}\right) h \bar{\nu}_c - \frac{1}{2} h \delta \left(n + \frac{1}{2} + m_s\right)^2.$$

circuit that is amplified and fed back to drive the oscillation. QND couplings of spin and cyclotron energies to $\bar{\nu}_z$ [6] arise because saturated nickel rings [Fig. 2(a)] produce a small magnetic bottle, $\Delta\mathbf{B} = \beta_2[(z^2 - \rho^2/2)\hat{\mathbf{z}} - z\rho\hat{\boldsymbol{\rho}}]$ with $\beta_2 = 1540\ \mathrm{T/m^2}$.

Anomaly transitions are induced by applying potentials oscillating at $\bar{\nu}_a$ to electrodes, to drive an off-resonance axial motion through the bottle's $z\boldsymbol{\rho}$ gradient. The electron sees the oscillating magnetic field perpendicular to **B** as needed to flip its spin, with a gradient that allows a simultaneous cyclotron transition. Cyclotron transitions are induced by microwaves with a transverse electric field that

Need to add relativistic corrections

δ: relativistic corrections

How to measure energy transitions in a Penning trap?

1. Work at very low temperatures → ground state is mainly populated
2. Indtroduce transition via external excitation
   - external micro-wave: excitation of cyclotron trasitions (n=0 → n=1)
   - spin-flip via oscillation of quadrupol potential (m=1/2 → m=-1/2)
3. Observe at which frequencies transition happens
   mirror charge at electrode indicates change in axial frequency ν_z
   (quantum nonmodolation measurement)

$$\Delta \nu_z = \delta \left(n + m_s \right)$$

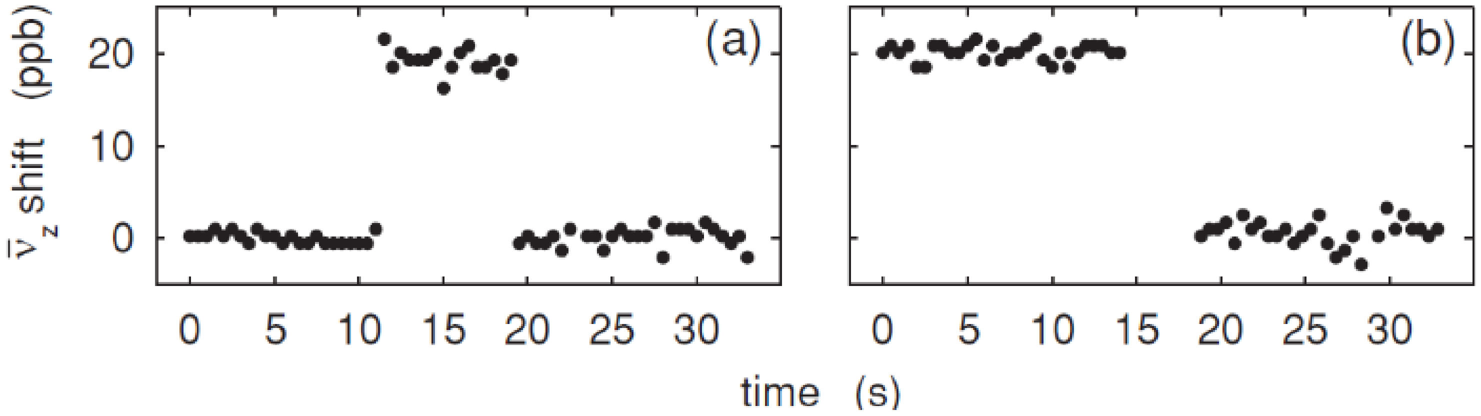

cyclotron transition

spin flip

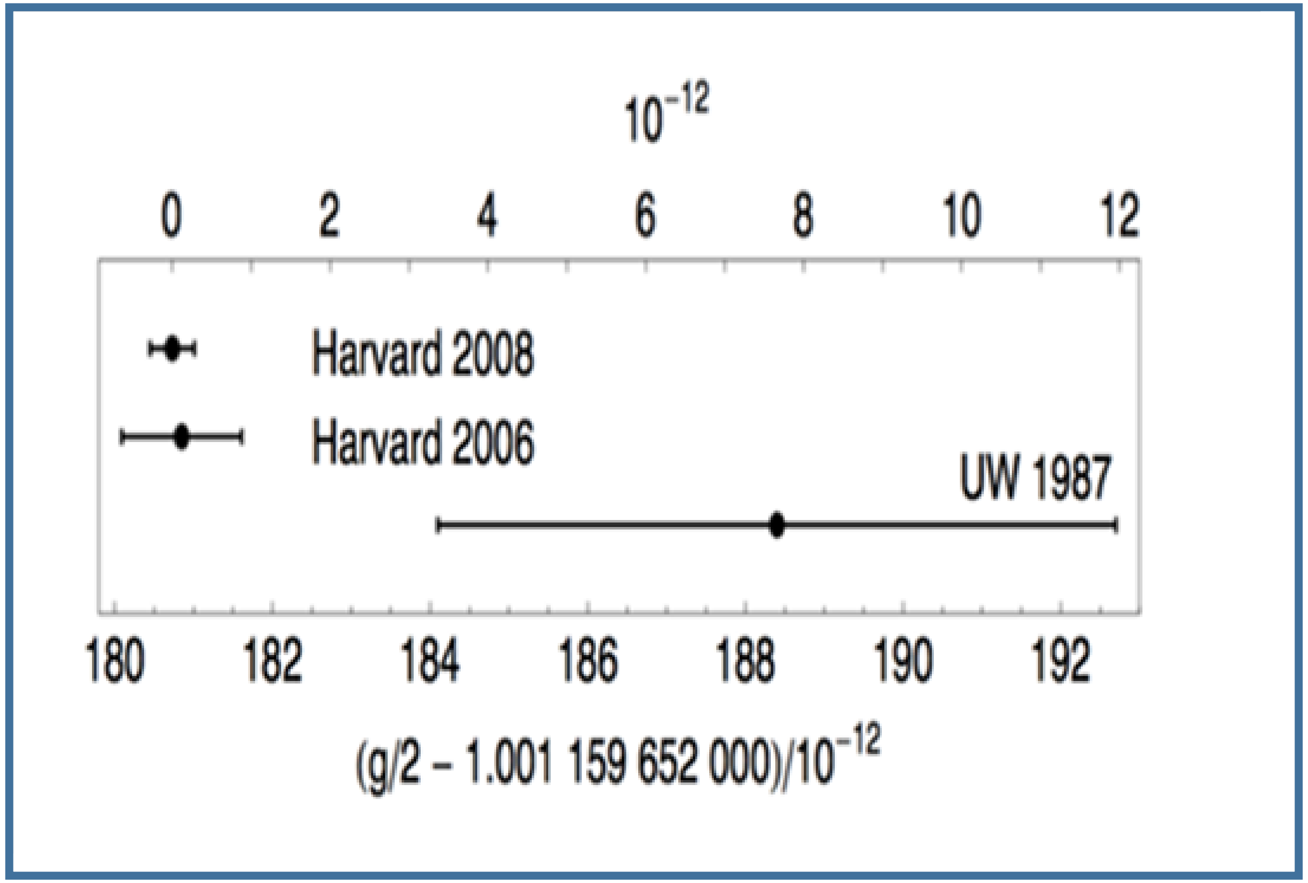

g/2 = 1.001 159 652 180 73 (28) (measured)

g/2 = 1.001 159 652 177 60 (520) (predicted)

Most precise test of QED!

Weak interaction

1. Phenomenology of weak decays
2. Parity violation and neutrino helicity
3. V-A theory
4. Neutral currents

The weak interaction **was** and **is a topic** with a lot of **surprises:**

Past: Flavor violation, P and CP violation.
Today: Weak decays used as probes for new physics

1. Phenomenology of weak decays

All particles (except photons and gluons) participate in the weak interaction. At small q^2 weak interaction can be shadowed by strong and electro-magnetic effects.

- Observation of weak effects only possible if strong/electro-magnetic processes are forbidden by conservation laws.
- Today's picture for charge current interaction is the **exchange** of **massive W-bosons** coupling only to **left-handed fermion currents**

$$\mu^- \to \bar{\nu}_\mu + e^- \bar{\nu}_e$$

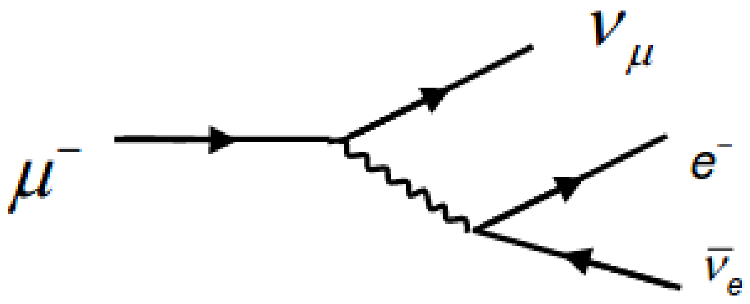

$$\tau = 2.6 \cdot 10^{-6} \text{s}$$

Electromagnetic decay $\mu^- \to e^- \gamma$ forbidden by lepton number conservation

Application of Feynman-rules for massive W bosn and LH coupling:

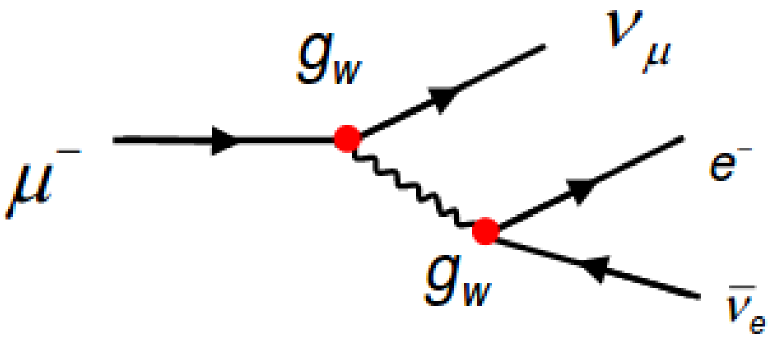

$$M = [\frac{g_w}{\sqrt{2}}\overline{u}_\nu \gamma^\mu \underbrace{\frac{1-\gamma^5}{2}}_{P_L} u_\mu] \frac{g_{\mu\nu} - q_\mu q_\nu / M_W^2}{q^2 - M_W^2} [\frac{g_w}{\sqrt{2}}\overline{u}_e \gamma^\mu \underbrace{\frac{1-\gamma^5}{2}}_{P_L} v_\nu]$$

„weakness“ results from $1/M_W^2$ supression

$$\alpha_{em} = \frac{1}{137} \qquad g_W = \frac{1}{40}$$

Fermi interaction

Non local current – current coupling

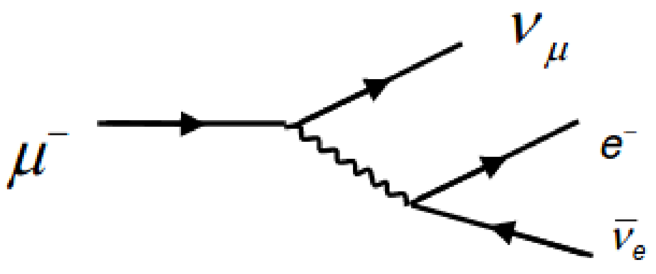

Point-like 4-fermion interaction

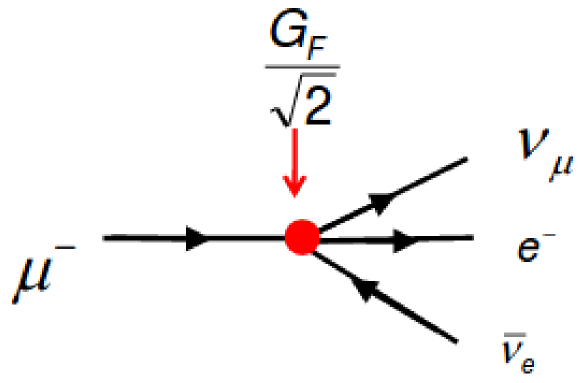

Fermi coupling constant, dimension = $(1/M)^2$

$$M = \frac{g_w^2}{8M_W^2}[\overline{u}_\nu \gamma^\mu (1-\gamma^5) u_\mu][\overline{u}_e \gamma^\mu (1-\gamma^5) v_\nu]$$

- 4-fermion theory is an **effective theory** valid for small q^2. Gives reliable results for most low energy problems.
- Conceptual problems in the high-energy limit (see later)
- Introduced by Fermi in 1933 to explain nuclear β decay.

$$\frac{G_F}{\sqrt{2}} = \frac{g_w^2}{8m_W^2}$$

Fermi's treatment of nuclear β-Decay: $n \to p\, e^- \,\bar{\nu}_e$

Fermi's explanation (1933/34) of the nuclear β-decay:

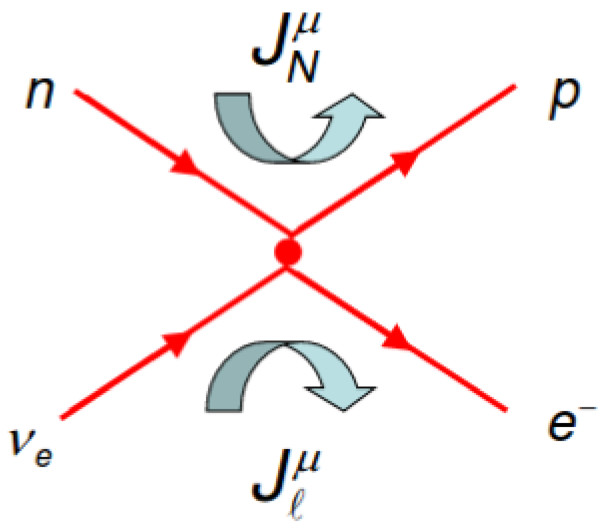

Two fermionic vector currents coupled by a **weak coupling const.** at single point (4-fermion interact.)

Apply "Feynman Rules"

$$M = \frac{G_F}{\sqrt{2}} \cdot J_{N,\mu} \cdot J_e^{\mu^+} = \frac{G_F}{\sqrt{2}} \cdot \left(\bar{u}_p \gamma_\mu u_n\right) \cdot \left(\bar{u}_e \gamma_\mu v_\nu\right)$$

Weak coupling constant G_F is a very small number ~10^{-5} GeV^{-2}.
Explains the "weakness" of the force.

Fermi's ansatz was inspired by the structure of the electromagnetic interaction and the fact that there is essentially no energy dependence observed.

Problem: Ansatz cannot explain parity violation (was no a problem in 1933)

Universality of weak coupling constant:

$\mu^- \rightarrow \bar{\nu}_\mu + e^- \bar{\nu}_e$

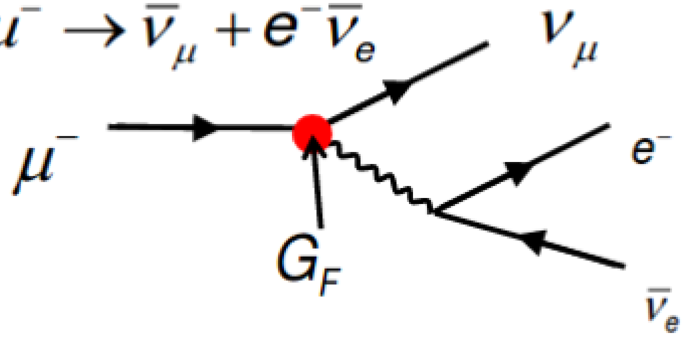

$\pi^- \rightarrow \mu^- \bar{\nu}_\mu$

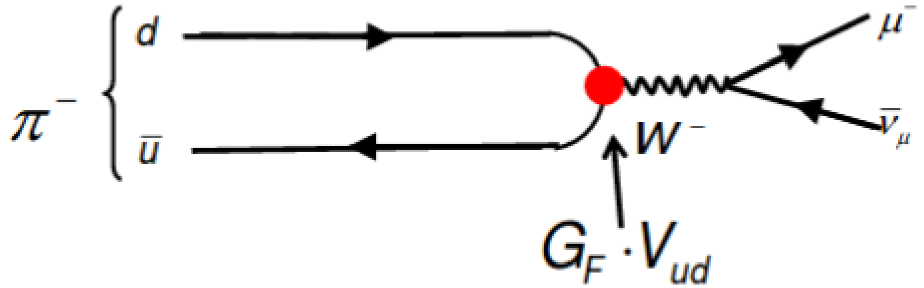

$K^- \rightarrow \mu^- \bar{\nu}_\mu$

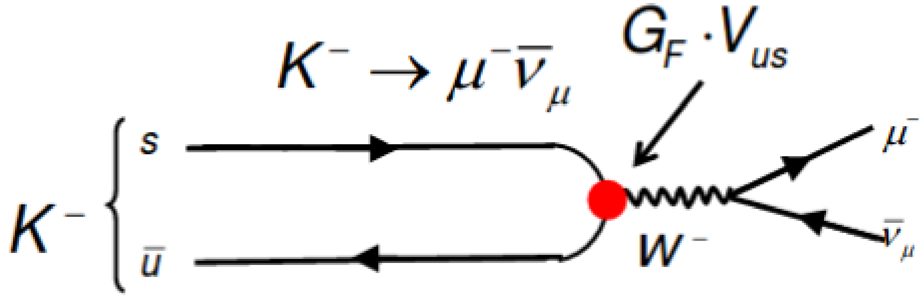

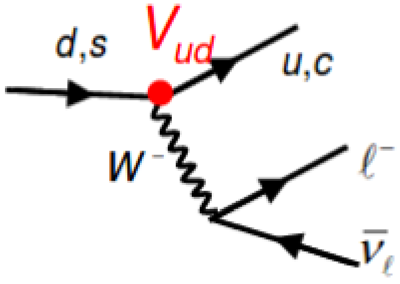

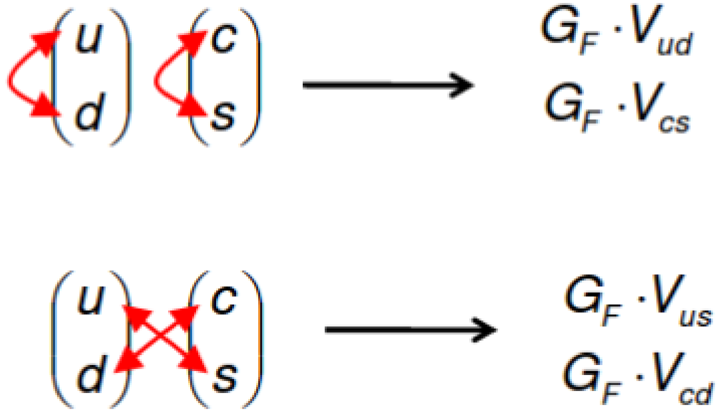

If one considers the quark mixing the weak coupling constant G_F is universal.

2. Parity violation and neutrino helicity

Historical Θ/τ

In 1956, parity conservation as well as T and C symmetry was a "dogma"

$\rightarrow$ very little experimental tests done

θ/τ puzzle:

$\theta \rightarrow \pi^+\pi^0$; P($\pi^+\pi^0$) = +1

$\tau \rightarrow \pi^+\pi^+\pi^-$; P($\pi^+\pi^+\pi^-$) = -1

P(q) = 1; P($\bar{q}$) = -1;

P(meson) = $P_q P_{\bar{q}}(-1)^L$;

lowest energy, $S = 0$

P=-1

θ, τ have same mass, same lifetime, however different parity ...

Yang, Lee:

$\rightarrow \theta = \tau = K^+$

weak interaction violates parity

proposed a set of measurements which test parity

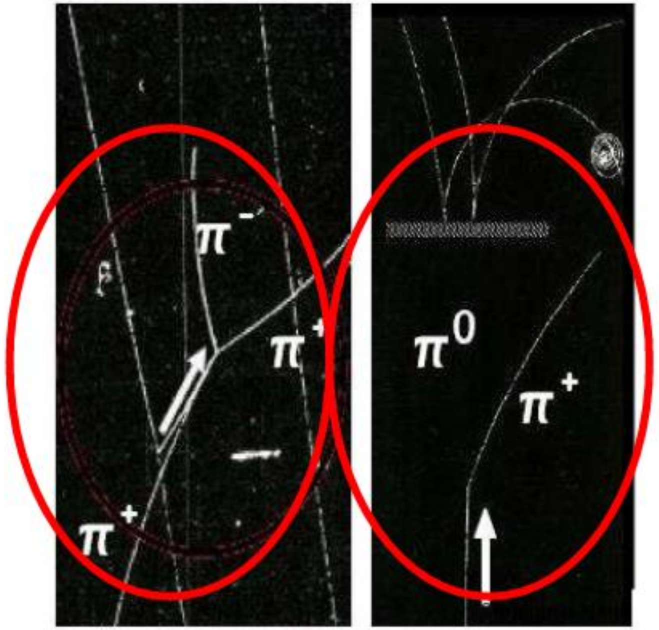

Wu-Experiment

Partiy conservation: physics stays invariant under parity conservation

Idea: Check that number of electrons emitted in direction of spin ($\vec{J}$) of ^{60}Co and in opposite direction (-$\vec{J}$) are the same.

$$^{60}Co \rightarrow ^{60}Ni^* + e^- + \overline{\nu_e}$$

$$P(\vec{J}) = P(\vec{r}\ x\ \vec{p}) = (-\vec{r})\ x\ (-\vec{p}) = \vec{J}$$

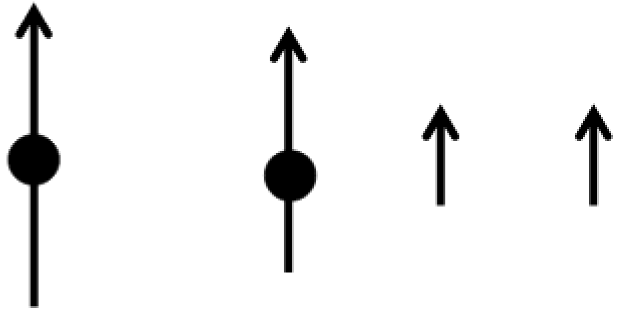

J=5 J=4

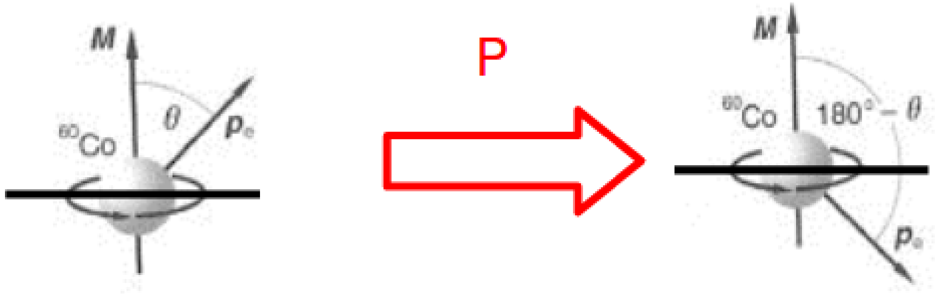

Experiment: Invert polarization of ^{60}Co and compare electron rate in same angle Θ

$$Ni^* \rightarrow Ni + \gamma$$

photons are preferentially emitted in direction of spin. Use photon distribution to test polarization of ^{60}Co. (elm IA conserves parity)

MAIN CHALLENGE: Polarization of ^{60}C0

Spin of ^{60}Co: J=5 → M = -5,-4, …., 4, 5

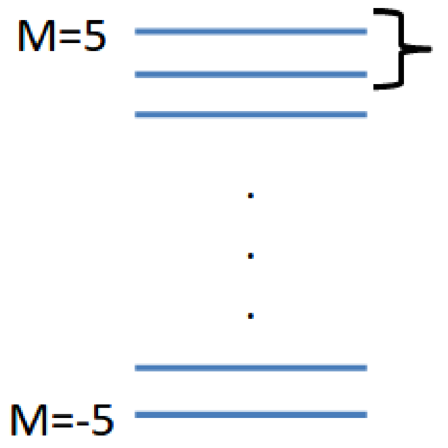

$\Delta E = g\, \mu_K\, B$

$\mu_K \sim 5.05 \times 10^{-27}$ J/T

Population of energy levels follows Boltzmann distribution:

$$e^{-\frac{E}{k_B T}}$$

for ΔE >> $k_B T$ only lowest energy level is populated, however for given B field in experiment (2.3 T) very low temperatures needed

g factor depends on gitter structure

Example: g= 7.5 (^{60}Co), B = 2.3 T, T = 0.003 K

$$\frac{P(m{=}-4)}{P(m{=}-5)} = e^{-\frac{\Delta E}{k_B T}} = 0.074$$ → 92% polarized ^{60}Co

Solution Part-I: embedding ^{60}C0 in a paramagnetic material (B ~ μ_r ; μ_r ~ 3-4)
still temepratures of T=0.01K needed

Wu-Experiment

Related to cooling

Requirements:

- 2 B fields in orthogonal directions

- detection of emitted electron
  (cover a small opening angle Θ)

- detection of emitted gamma
  (to test polarization of ^{60}Co)

- crystal needs to be located
  in helium bath first than in vacuum

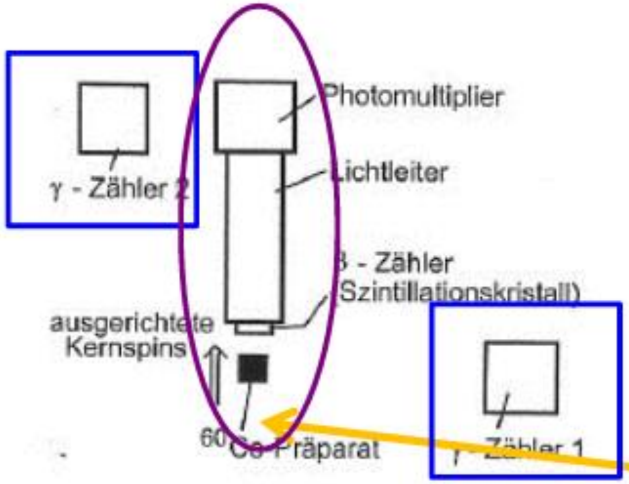

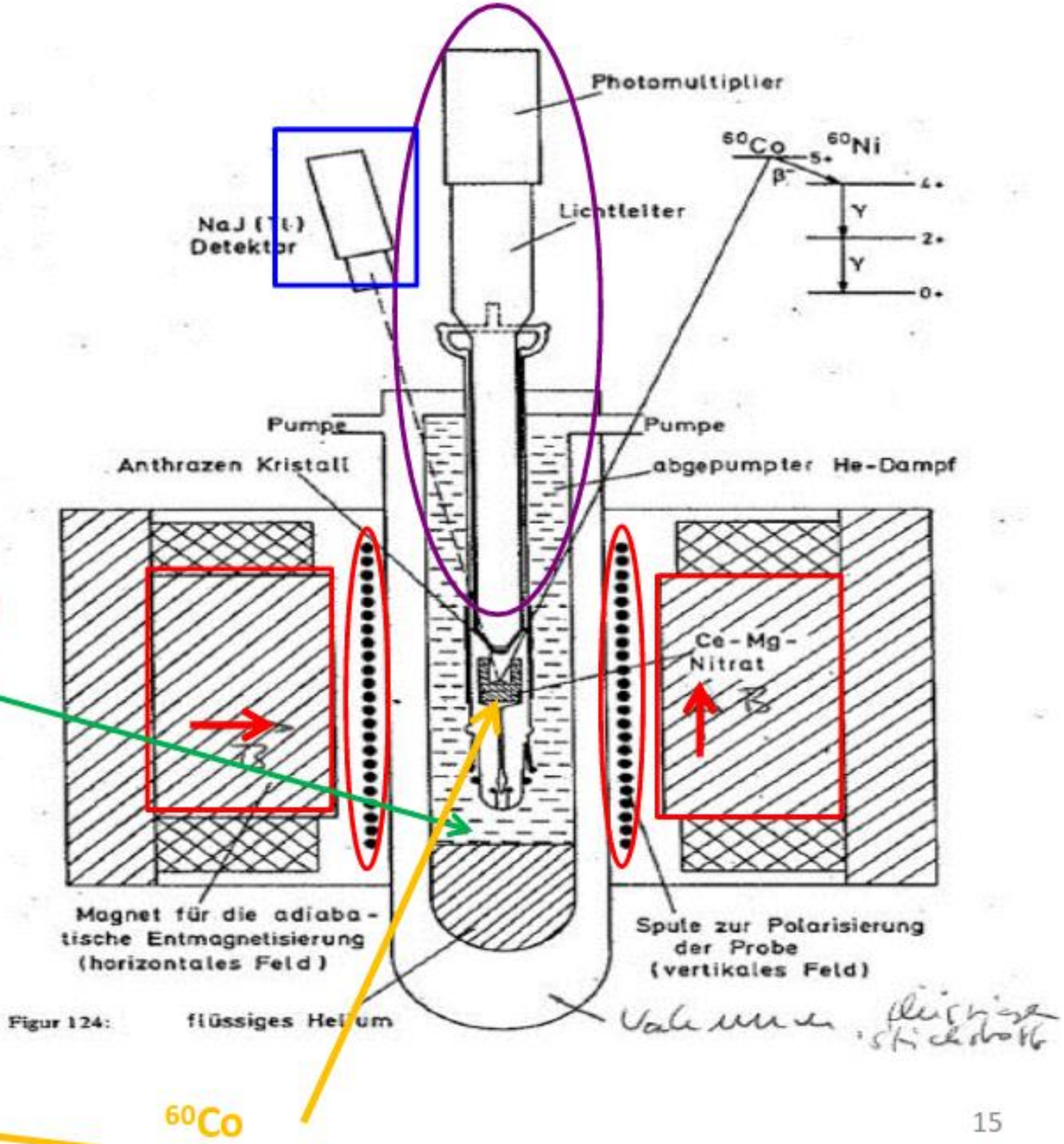

Wu-Experiment: Results

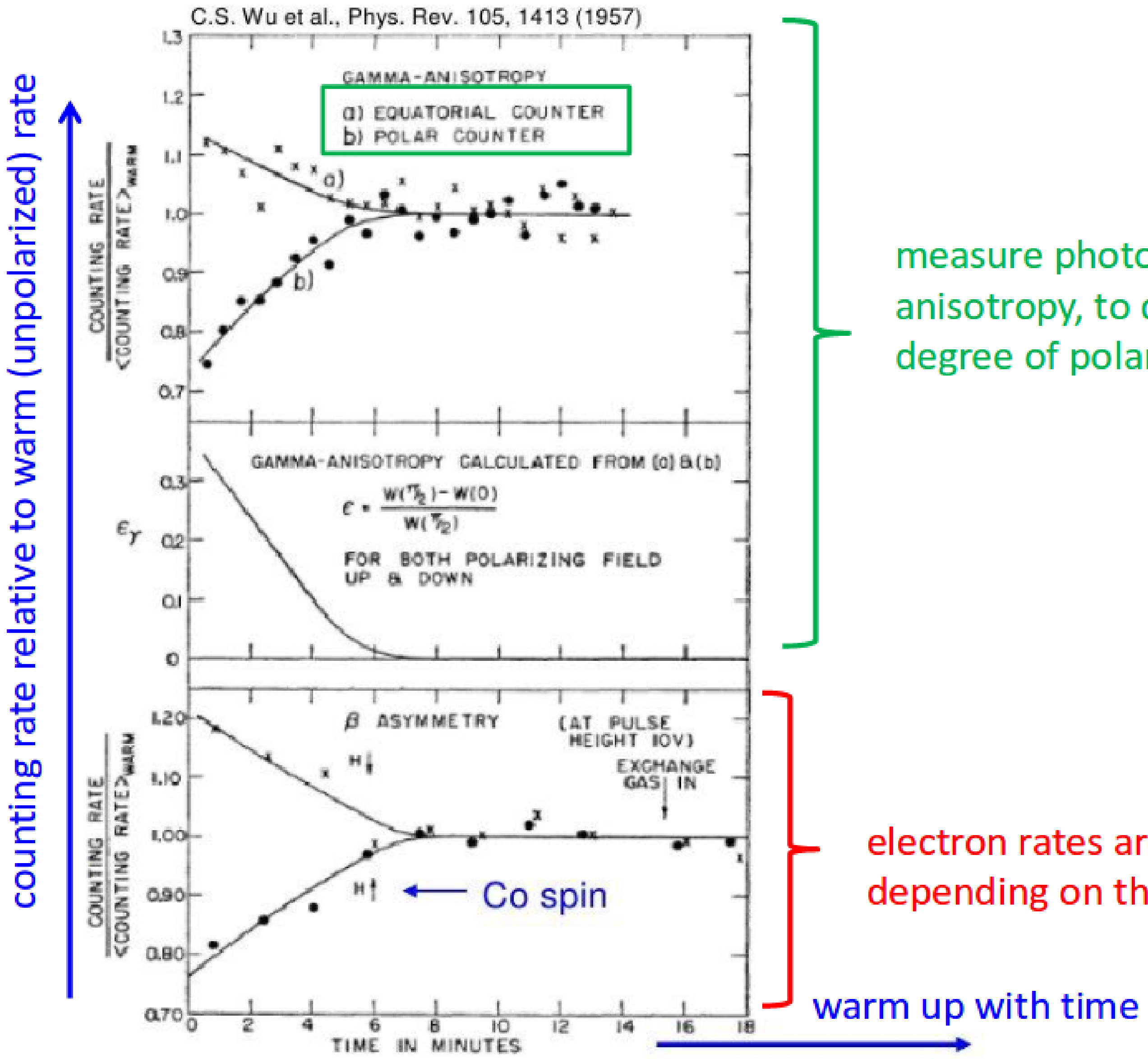

measure photon anisotropy, to determine degree of polarization

electron rates are different depending on the polarization!

→ **Parity violation!**

Qualitative Explanation

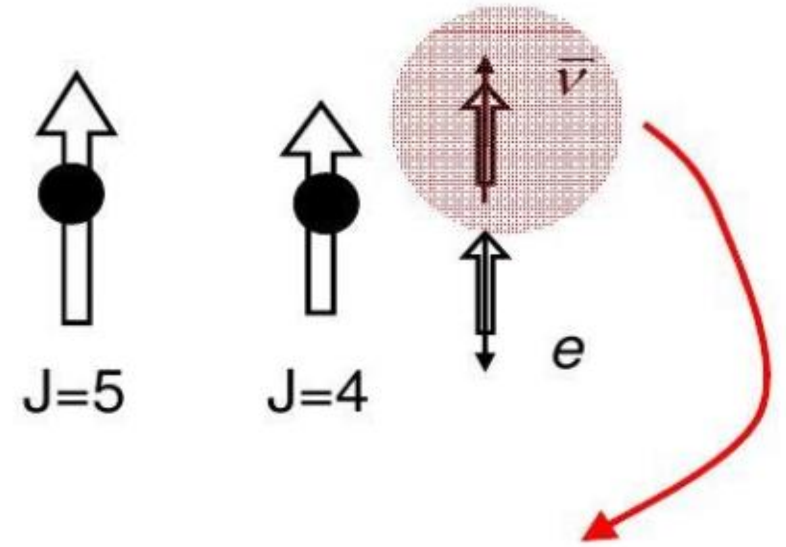

Consequence of existence of only left-handed (LH) neutrinos (RH anti-neutrinos)

Wu experiment established CP violation!

It was however not precise enough to measure helicity of neutrino
H ~ 0.7 ± large uncertainties

→ Goldhaber experiment

Goldhaber Experiment

$^{152}Eu + e^- \rightarrow {}^{152}Sm^* + \nu_e$

$\hookrightarrow {}^{152}Sm + \gamma$

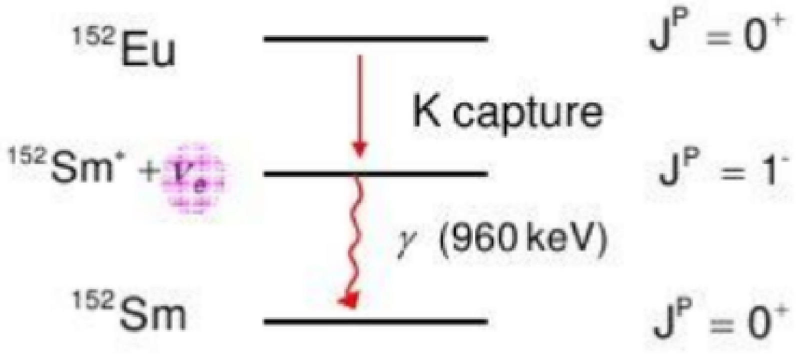

Light blue and green arrows indicate possible spin configurations

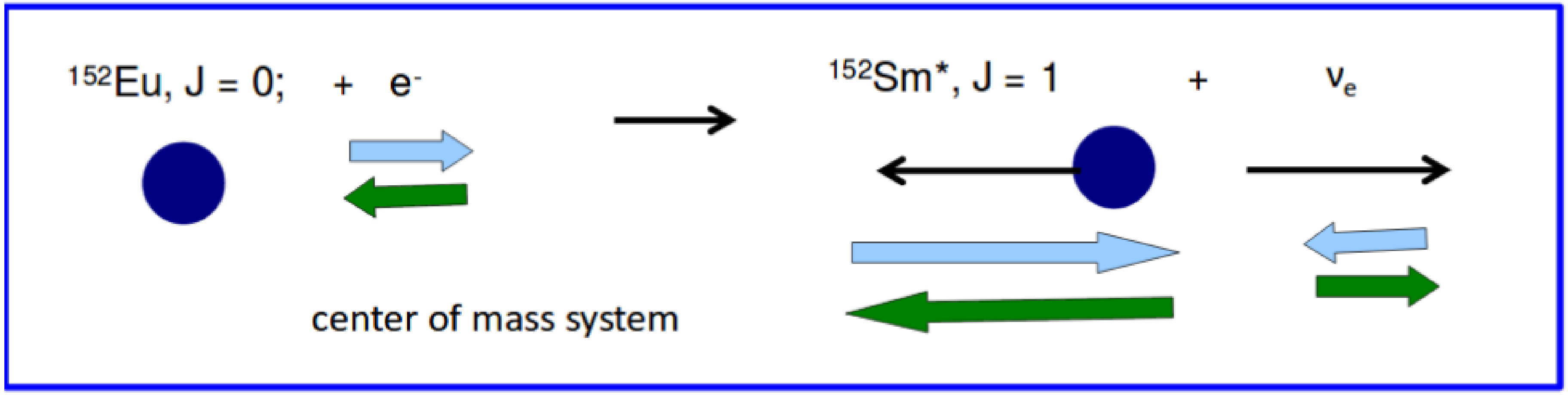

spin of neutrino is in opposite direction than the one of $^{152}Sm^*$,
momentum of is in opposite direction than the one of $^{152}Sm^*$

Goldhaber Experiment

$^{152}Eu + e^- \rightarrow {}^{152}Sm^* + \nu_e$

$^{152}Sm^* \rightarrow {}^{152}Sm + \gamma$

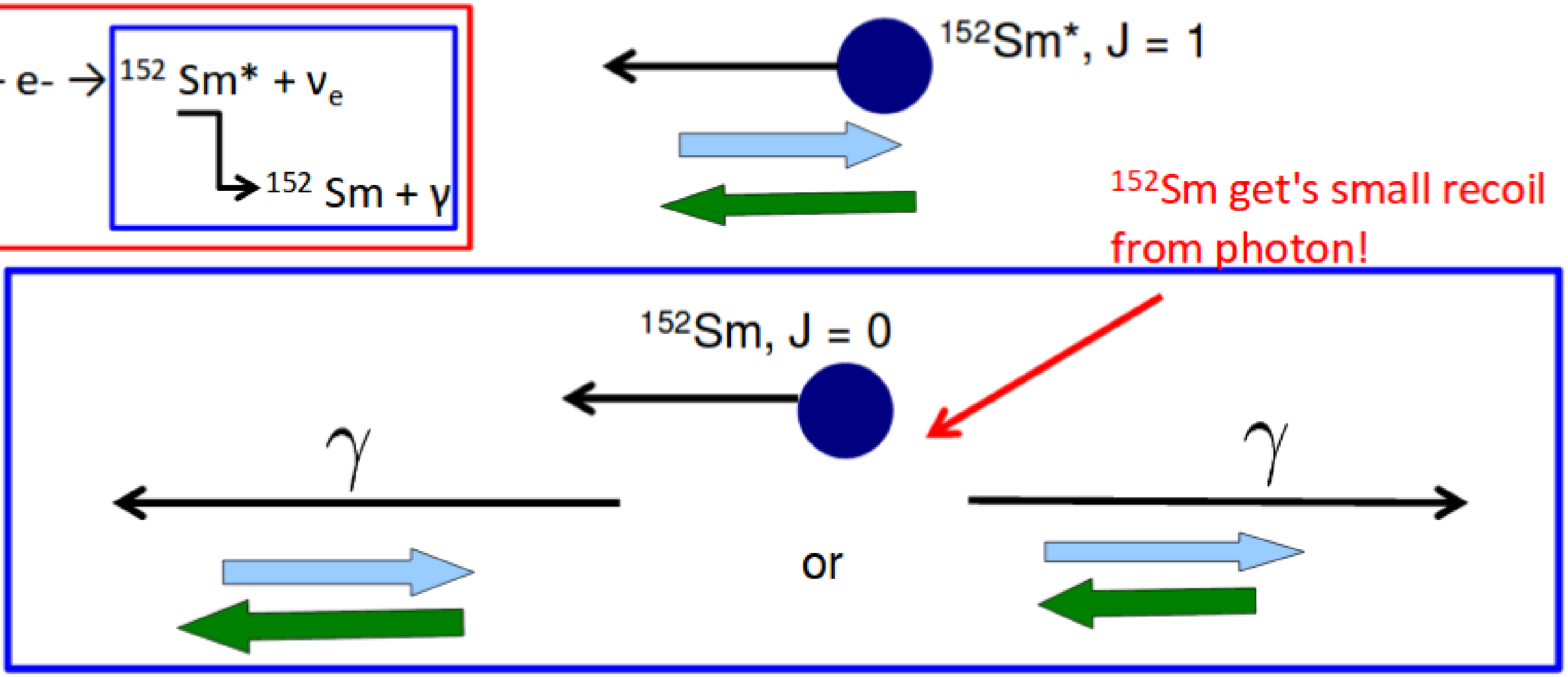

direction of spin of photon is opposite of neutrino

emitted in direction of Sm*

$$h(\gamma) = h(\nu_e)$$

emitted in opposite direction of Sm*

$$h(\gamma) = -h(\nu_e)$$

Two open question: 1) What is the direction of emission of the photon?

2) What is the polarization of the photon?

Resonant Scattering

To compensate the nuclear recoil, the photon energy must be slightly larger than 960 keV.

This is the case for photons which have been emitted in the direction of the Eu→Sm recoil (Doppler-effect).

Resonant scattering only possible for "forward" emitted photons, which carry the polarization of the Sm^* and thus the polarization of the neutrinos.

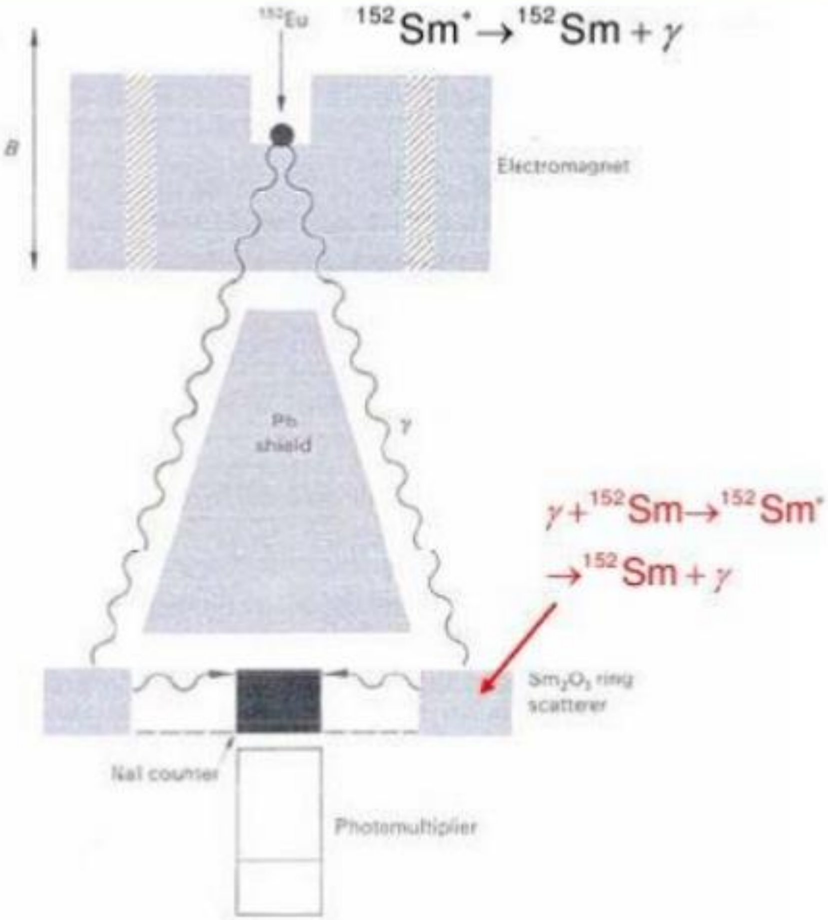

Fig. 7.8. Schematic diagram of the apparatus used by Goldhaber *et al.*, in which γ-rays from the decay of $^{152}Sm^*$, produced following K-capture in ^{152}Eu, undergo resonance scattering in Sm_2O_3 and are recorded by a sodium iodide scintillator and photomultiplier. The transmission of photons through the iron surrounding the source depends on their helicity and the direction of the magnetic field **B**.

Measurement of Polarization of Photon

Exploit that the transmission index through magnetized iron is polarization dependent: Compton scattering in magnetized iror

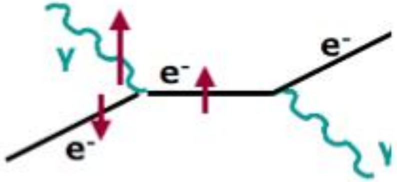

iron in B field

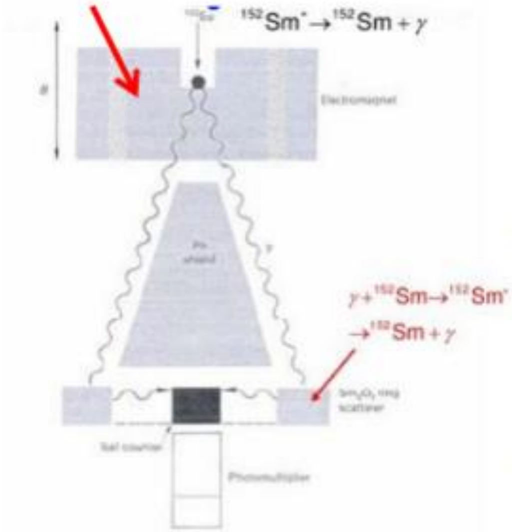

γ	γ
.H ⇐	RH ⇒
$\vec{B}$ ⇒	$\vec{B}$ ⇒
Polarization of electrons in iron ⇐	Polarization of electrons in iron ⇐
(.. minimize pot. energy)	Absorption leads to spin flip
⬇	⬇
LH photons cannot be absorbed: Good transmission	RH photons undergo Compton scattering: Bad transmission

Photons w/ polarization anti-parallel to magnetization undergo less absorption

Goldhaber Experiment: Result

- Due to geometry of experiment, only resonant scattered photons are detected
  Helicity of detected photons identical to helicity of neutrino.

- Detect photons which pass trough magnetized iron.

B field points in flight direction of photons
→ measure fraction of (mainly) LH photons

B field points in opposit direction
→ measure fraction of (mainly) RH photons

$$\delta = \frac{N_{-} - N_{+}}{0.5(N_{-} + N_{+})} = 0.017 \pm 0.003$$

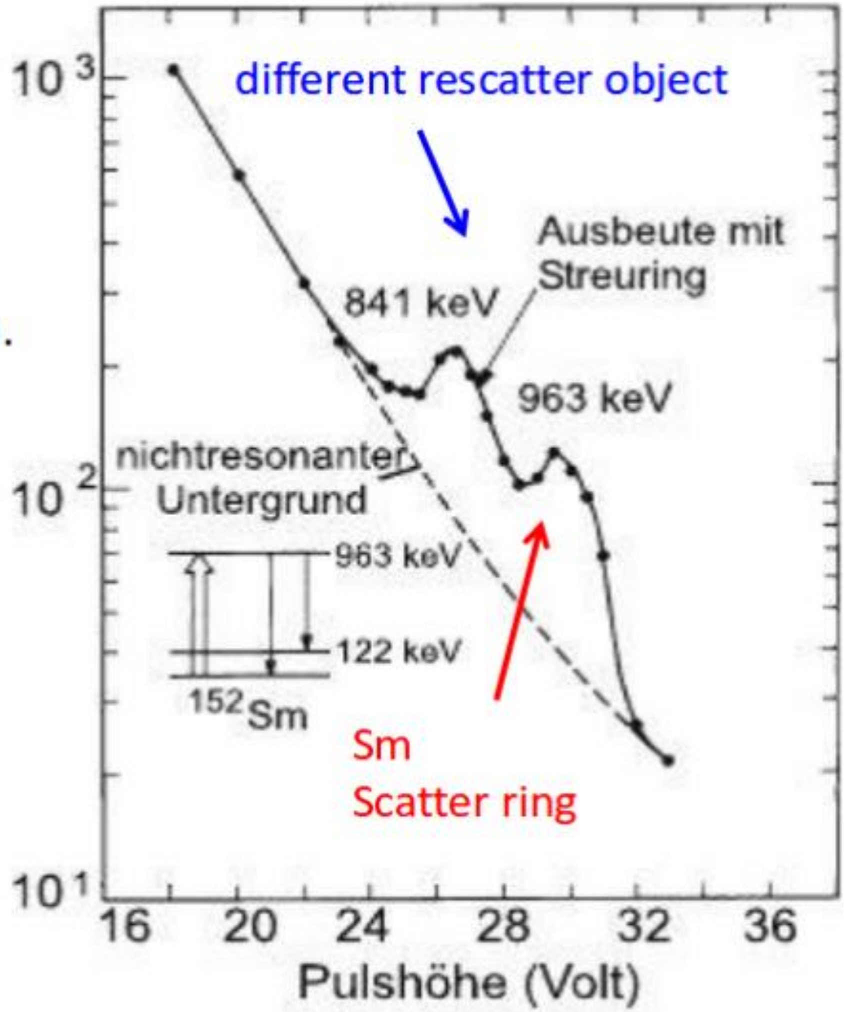

N_ : counting rate with magentic field down
N_+: counting rate with magnetic field up

Goldhaber-Experiment: Result

Result: $\delta = +0.017 \pm 0.003$

Theoretical expectation (for 100% polarized photons)

$$\delta = \pm 0.025 \begin{cases} \text{„-“ for } h > 0 \\ \text{„+“ for } h < 0 \end{cases}$$

Only 5-8% of electrons in iron are polarized, thus asymmetry of scattering for LH and RH photons is very small, thus heavily wash out the asymmetry.

Due to background effects (thermal movements inside the source, polarisation can depend on angle, …) expect for pure LH neutrios 75% polarized photons

Measured photo polarisation: 66 ± 15%, consistent with 75%

→ **Neutrino are left handed particles**